CHAPTER 7

ENERGY AND POWER DERIVATIVES

SECTIONS

The pricing of energy and power derivatives are reviewed in detail in this chapter. In §7.1, we discuss electricity markets. In §7.2, we review electricity pricing models including both one-factor and two-factor models, jump diffusion models, and stochastic volatility models. Estimation of model parameters is also discussed. In §7.3, we discuss electricity swing options. In §7.4, we review the Longstaff-Schwartz algorithm of least-squares Monte Carlo (LSM) for pricing American and Bermudan options. In §7.5, we then extend the application of LSM to pricing swing options based on the work of Doerr (2003) and

Meyer (2004). In §7.6, we incorporate upswings, downswings, and penalty functions, general features of swing options, into the LSM pricing algorithm. In §7.7, a swing option pricing implementation in Matlab of Doerr is provided. In §7.8, LSM simulation results are provided from the work of Doerr (2003). In §7.9, we discuss the pricing of energy commodity derivatives including cross-commodity spread options, as well as crack and spark spread options. In §7.10, we discuss jump diffusion models for pricing electricity derivatives, while in §7.11, we discuss stochastic volatility electricity pricing models. In §7.12, we discuss parameter estimation of the pricing models in §7.10 and §7.11 based on the work of Xiong (2004). Estimation methods like maximum likelihood (ML), generalized method of moments (GMM), ML of the conditional characteristic function (CCF), and spectral generalized method of moments (SGMM) are discussed. In §7.13, the parameter estimation methodology of Xiong (2004) is provided in Matlab. In §7.14, we review general energy commodity pricing models. We discuss natural gas derivatives, giving an overview of the market, in §7.15 and discuss pricing models based on the work of Xu (2004) in §7.16. In §7.17, a natural gas pricing implementation in Matlab of Xu is given. Finally, in §7.18, we discuss natural gas and electricity swaps.

7.1 Electricity Markets

Electricity, like weather, is characterized by its non-storability, in addition to its very limited transportability, making electricity delivered at different times and on different dates to be perceived by consumers as distinct commodities. On-peak and off-peak demand for electricity at different time periods (i.e., seasons) has a significant impact on electricity prices and is important in power markets as they determine, for instance, derivative contractual terms. Electricity prices are strongly dependent on the electricity needs (demand) of consumers and their determinants, including business activity and temporal weather conditions.

The non-storability and limited transportability of electricity affects the ability of "carrying" electricity across time and space and is essential in explaining the behavior of electricity spot and forward derivative prices as compared to other commodities. In other words, "arbitrage across time and space, which is based on storability and transportation, is seriously limited, if not completely eliminated, in electricity markets."[1] One would expect spot prices to be highly dependent on temporal and local supply and demand conditions if the links across time and space provided by arbitrage break down.[2]

Thus, the limits of arbitrage would be expected to affect decisively the relationship between spot and forward prices. Non-storability implies that arbitrage arguments cannot be used in defining a pricing model when electricity, like weather, is the underlying asset of a derivative contract. As a result, cost-of-carry models do not work (see Geman and Roncoroni [2001]) because they cannot capture the physical and temporal constraints of electricity as a non-storable commodity.

Transportation constraints on electricity are imposed by capacity limits of transmission lines and transportation loads, which can make transmission of electricity to certain regions impossible or uneconomical. The supply of electricity is also based on the availability of transportation line connections, which can be damaged by rare and extreme events such as power plant failures—e.g., the occurrence in August 2003 that led to severe power outages

in the Midwest and Northeast. Such power failures can lead to dramatic price spikes. In the summer of 1998, the spot price of electricity in Eastern and Midwestern U.S. skyrocketed from \$50/MWh to \$70/MWh because of unexpected unavailability of some power generation plants and congestion on key transmission lines. As an example, consider Figure 7.1, which shows the historical on-peak electricity spot prices in Texas (ERCOT) and at the California and Oregon border (COB). The jumpy behavior in electricity spot prices is mainly attributed to the fact that "a typical regional aggregate supply function of electricity almost always has a kink at certain capacity levels and the supply curve has a steep upward slope beyond that capacity level."[3]

Figure 7.2 shows a comparison of wholesale electricity prices from 1999 to 2002 in the Midwest (ECAR) and Pennsylvania-Maryland-New Jersey (PJM) regions, the California-Oregon border, and at Palo Verde, a major hub for importing electricity into California, which show a large number of "spikes" in summer months.

These limitations make electricity contracts and prices "highly local; i.e., strongly dependent on the local determinants of supply and demand (such as characteristics of local generation plants, and local climate and weather conditions together with their derived uses of electricity)."[4] Given the non-storability and transportation limitations of electricity, derivative pricing is usually done in an incomplete market framework.

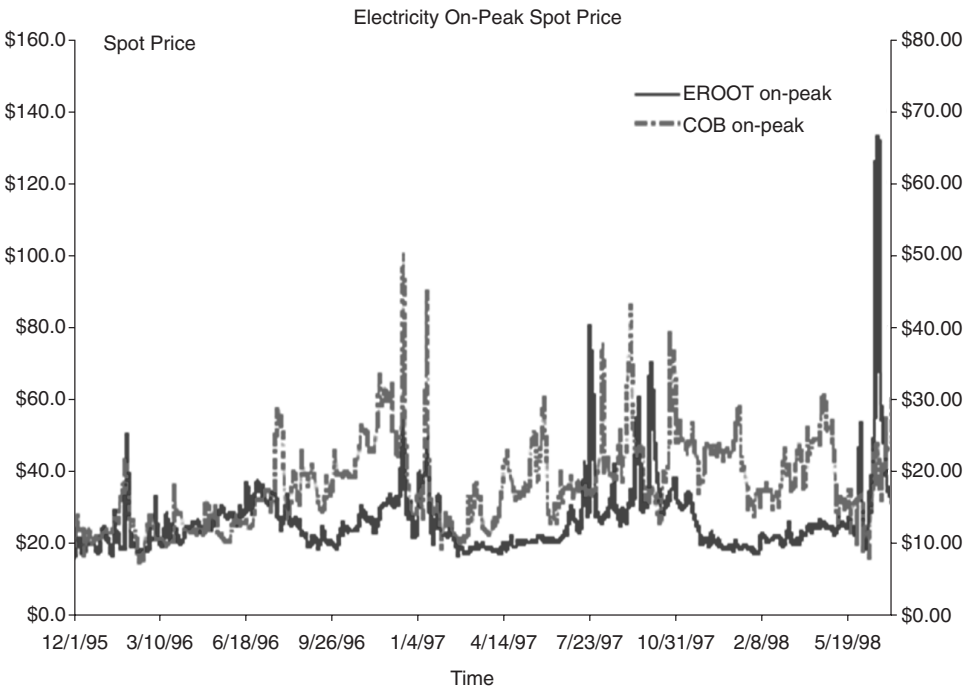

Figure 7.1 ERCOT and COB on-peak electricity spot prices.

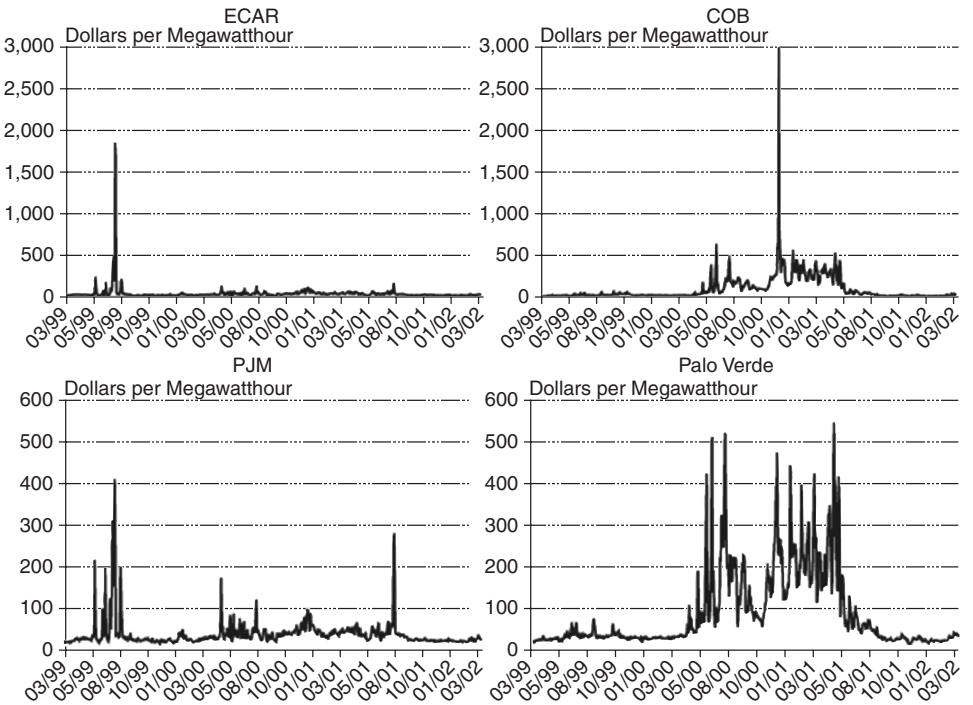

Figure 7.2 *Source: Commodity Futures Trading Commission (see Energy Information Administration, EIAGIS-NG Geographic Information System).*

The deregulation of the energy market has led to competitive wholesale electricity markets and has been accompanied by power derivative contracts, both OTC and exchange-traded, providing a variety of contract provisions to meet the needs of electricity market participants. In the U.S., electricity futures and options contracts have been listed in recent years by the Chicago Board of Trade (CBOT), the New York Mercantile Exchange (NYMEX), and the Minneapolis Grain Exchange.[5] The demand for these contracts has increased based on the increased forecasted demand for energy and investment in power generators. The Energy Information Administration (EIA) forecasts that meeting U.S. demand for electricity over the next decade will require about 198 gigawatts of new generating capacity.[6]

7.2 Electricity Pricing Models

Modeling the Price Process

Energy prices are mostly driven by supply and demand. Together with some characteristic properties of electricity, such as its heterogeneous nature with respect to time and location of its generation, its non-storability, and the incomplete market for electricity given arbitrage technical constraints, electricity spot prices exhibit pronounced short-term volatil-

ity. In addition, electricity prices exhibit the following properties that result from the peculiarities of supply and demand: mean-reversion, cyclical variations, and occasional prices spikes.

With mean-reversion, volatility decreases with increasing time horizon. There is a long-term equilibrium ("fair price") that is much less volatile than the spot price. The mean-reversion speed is determined by how quickly supply can react to sudden demand change (see Pilipovic (1998)).[7] Cyclical variations occur on different time-scales (time of day, day of week, seasons) and are driven by cyclical demand changes. This aspect of the price process can be considered deterministic and therefore can be easily separated from the stochastic time dependence.[8] Price spikes (surges) occasionally occur in addition to the large short-term volatility, but last only for a short time. Positive spikes can be caused by outages in the generation or transmission process (see Eydeland and Geman [1999]), while negative spikes occur when it is difficult to reduce generation capacity in periods of low demand.

Given these observations, simple geometric Brownian motion is not well suited to modeling electricity price processes because they do not capture spikes. Therefore, jump diffusion processes are frequently used. For instance, a discrete jump diffusion component can be added to a log-normal model. One-factor and two-factor lognormal mean-reverting processes with jumps have been proposed. We will examine the one-factor model.

One-Factor Model

Denote the spot price for electricity S_t. The stochastic process can be represented as the sum of two components—a deterministic function of time, $f(t)$, and a diffusion stochastic process, X_t, of a state variable (e.g., power load). That is,

$$S_t = f(t) + X_t. \tag{7.1}$$

We assume that X_t follows a stationary mean-reverting Ornstein-Uhlenbeck process:

$$dX_t = -\kappa X_t dt + \sigma dW_t \tag{7.2}$$

where $\kappa > 0$ is the speed of mean-reversion, $X(0) = x_0$, and dW_t represents an increment to a standard Brownian motion. Because $X_t = S_t - f(t)$, and assuming that the function $f(t)$ satisfies the appropriate regularity conditions, we can write (7.1) and (7.2) as

$$d(S_t - f(t)) = \kappa(f(t) - S_t)dt + \sigma dW \tag{7.3}$$

which shows that when S_t deviates from the deterministic term $f(t)$, it is pulled back at a rate proportional to its deviation. In this model, the only source of uncertainty comes from the stochastic behavior of X_t as described by (7.2).

Following Lucia and Schwartz (2001), the process followed by S_t can be expressed as the solution of the stochastic differential equation (provided that the function $f(t)$ satisfies the appropriate regularity conditions, such as $\int_{-\infty}^{\infty} f(t)^2 dt < \infty$ —i.e., the function is bounded), as follows:

$$dS_t = \kappa(\alpha(t) - S_t)dt + \sigma dW \tag{7.4}$$

where $\alpha(t)$ is the deterministic function of t defined by:

$$\alpha(t) = \frac{1}{\kappa}\frac{df(t)}{dt} + f(t) \tag{7.5}$$

which can be viewed as a particular case of the extended Vasicek model.

The assumed simple one-factor model is analytically tractable. An explicit solution for (7.2), in conjunction with (7.1), yields:

$$S_t = f(t) + X_0 e^{-\kappa t} + \sigma \int_0^t e^{\kappa(s-t)} dW(s) \tag{7.6}$$

We find that the conditional distribution of E_t is normal with conditional mean and variance given by (using $X_0 = E_0 - f(0)$):

$$\begin{aligned} \mathrm{E}[S_t] &= \mathrm{E}[S_t|X_t] = f(t) + (S_0 - f(0))e^{-\kappa t} \\ \mathrm{Var}[S_t] &= \mathrm{Var}[S_t|X_0] = \frac{\sigma^2}{2\kappa}\left(1 - e^{-2\kappa t}\right),\ \kappa > 0 \end{aligned} \tag{7.7}$$

where $\mathrm{E}[\cdot]$ is the expectation operator.

The price process of S_t tends to a mean value of $f(t)$ in the long run, given its initial value of S_0. The higher the value of κ (assuming $\kappa > 0$), the faster the convergence. The variance, in turn, decreases with the time horizon and has a finite limit of $\sigma^2/2\kappa$ as the horizon tends to infinity.

To price electricity derivatives, we need the risk-neutral process under a martingale measure for the state variable X_t, instead of the real process under the physical measure in (7.2). Taking into account the non-tradable nature of X_t, standard arbitrage arguments with two derivative assets allow us to obtain the risk-neutral process for X_t. Under the change of measure using Girsonov's transformation, we change the drift by setting $dW^* = dW - \lambda dt$, so that

$$dX_t = \kappa\left(\alpha^* - X_t\right)dt + \sigma dW^* \tag{7.8}$$

where

$$\alpha^* = -\frac{\lambda\sigma}{\kappa} \tag{7.9}$$

and dW^* is an increment to W_t^*, a standard Brownian motion under the risk-neutral probability measure, and λ denotes the market price of risk linked to the state variable X_t. While we assume λ is constant, it could be a function of t and the state variable X_t.

The explicit solution for the SDE in (7.8) yields:

$$S_t = f(t) + X_0 e^{-\kappa t} + \alpha^*(1 - e^{-\kappa t}) + \sigma \int_0^t e^{\kappa(s-t)} dW^*(s) \tag{7.10}$$

with α^* as defined in (7.9). We find from this that S_t is conditionally normally distributed under the risk-neutral measure, with the following conditional mean:

$$\mathrm{E}^*[S_t] = f(t) + X_0 e^{-\kappa t} + \alpha^*(1 - e^{-\kappa t}) \tag{7.11}$$

We know that the value of any derivative security is its expected value of its payoff, under the risk-neutral measure, discounted back to the valuation date at the risk-free rate, which we assume to be constant. The value at time zero of a forward contract on the spot price of electricity maturing at time T must be:

$$V_0(X_t, T) = e^{-rT}\mathrm{E}_0^*[S_T - F_0(S_0, T)] \tag{7.12}$$

where $F_0(X_0, T)$ is the forward price set at time zero for a contract maturing at time T, and r is the riskless continuously compounded interest rate. Because the value of a forward contract must be zero when initially entered into, we finally derive the following closed-form solution for the forward (futures) price of electricity[9] using (7.11) and (7.1) for $t = 0$:

$$F_0(S_0, T) = \mathrm{E}_0^*[S_T] = f(T) + (S_0 - f(0))e^{-\kappa T} + \alpha^*(1 - e^{-\kappa T}) \tag{7.13}$$

with $\alpha^* = -\lambda\sigma/\kappa$.

Suppose the model in (7.1) is modified to incorporate the natural logarithm of the spot price instead of the spot price itself written as:

$$\ln S_t = f(t) + Y_t \tag{7.14}$$

so that

$$S_t = f(t)e^{Y_t}$$

where $f(t)$ is a known deterministic function of time, and Y_t is a stochastic process whose dynamics are given by:

$$dY_t = -\kappa Y_t dt + \sigma dW \tag{7.15}$$

with $\kappa > 0$ and $Y(0) = y_0$. The log-price follows a zero mean-reverting process, which implies the following price process under suitable conditions for $f(t)$:

$$dS_t = \kappa\left(b(t) - \ln S_t\right) S_t dt + \sigma S_t dW(t) \tag{7.16}$$

where

$$b(t) = \frac{1}{\kappa}\left(\frac{\sigma^2}{2} + \frac{d\log f(t)}{dt}\right) + \log f(t)$$

From (7.16), $\ln S_t$ has a conditional normal distribution with conditional mean and variance:

$$\begin{aligned}\mathrm{E}_0[S_t] &= \exp\left(\mathrm{E}_0[\ln S_t] + \frac{1}{2}\mathrm{Var}_0[\ln S_t]\right) \\ &= \exp\left(\left(f(t) + (\ln S_0 - f(0))\, e^{-\kappa t} + \frac{\sigma^2}{4\kappa}(1 - e^{-2\kappa t})\right)\right.\end{aligned}$$

and

$$\begin{aligned}\mathrm{Var}_0(S_t) &= \exp\left(2\mathrm{E}_0[\ln S_t] + \mathrm{Var}_0[\ln S_t]\right)\left(\exp\left(\mathrm{Var}_0[\ln S_t]\right) - 1\right) \\ &= \mathrm{E}_0[S_t]^2\left[\exp\left(\frac{\sigma^2}{2\kappa}(1 - e^{-2\kappa t})\right) - 1\right]\end{aligned}$$

After changing the log price process to the risk-neutral measure under Girsonov's theorem, similar to (7.8), it can be shown that the forward (future) of the log electricity price is:[10]

$$\begin{aligned}&F_0(S_0, T) \\ &\quad = \mathrm{E}_0^*[S_T] \\ &\quad = \exp\left[f(T) + (\ln S_0 - f(0))e^{-\kappa T} + \alpha^*(1 - e^{-\kappa T}) + \frac{\sigma^2}{4\kappa}\left(1 - e^{-2\kappa T}\right)\right]\end{aligned} \tag{7.17}$$

where $\alpha^* = -\lambda\sigma/\kappa$. Note that the deterministic component of the behavior of the spot price (log-price) appears directly in the price of the forward (futures) contracts (see (7.13) and (7.17)), that term "being an important determinant of the shape of the forward (futures) curve."[11] In both the one-factor and log-factor models, all forward (futures) prices are perfectly correlated.[12]

Estimating the Deterministic Component

In order to implement the models in (7.1) and (7.14), it is necessary to specify the deterministic time function $f(t)$. This function tries to capture any relevant predictable components of the electricity prices behavior arising from genuine regularities along time. Although there are various choices available, the chosen function should have a deterministic general trend and capture seasonal and cyclical behavior. For instance, as suggested by Pilipovic (1998), a sinusoidal function like the cosine function could be used to reflect the general seasonal pattern of the price time series.

Lucia and Schwartz (2001) suggest the following function:

$$f(t) = \alpha + \beta D_t + \gamma\cos\left((t + \tau)\frac{2\pi}{365}\right) \tag{7.18}$$

where

$$D_t = \begin{cases} 1 & \text{if date } t \text{ is weekend or holiday} \\ 0 & \text{otherwise} \end{cases}$$

and cos is the cosine function measured in radians, and α, β, γ, and τ are all constant parameters. Here, the coefficient β tries to capture the changes in the level of the variable for weekends and holidays where electricity usage typically increases. The cosine function is expected to reflect the seasonal pattern in the evolution of the relevant variable throughout the year and so has annual periodicity.

Estimation of the Stochastic Process for the One-Factor Models

To estimate the stochastic process for the one-factor model from the spot price data, we discretize (7.1):

$$X_t = (1-\kappa)X_{t-1} + \xi_t \tag{7.19}$$

for $t = 0, 1, 2, ..., N$, and where the innovations ξ_t are i.i.d normal random variables with mean 0 and variance σ^2. The same discretization can be used for the process Y_t in equation (7.15).

Given the discretization, we can estimate by the one-factor price and log-price models:

One-Factor Model

$$\begin{aligned} S_t &= \alpha + \beta D_t + \gamma \cos\left((t+\tau)\frac{2\pi}{365}\right) + X_t \\ X_t &= \phi X_{t-1} + u_t \end{aligned} \tag{7.20}$$

One-Factor Log Price Model

$$\begin{aligned} \ln S_t &= \alpha + \beta D_t + \gamma \cos\left((t+\tau)\frac{2\pi}{365}\right) + Y_t \\ Y_t &= \phi Y_{t-1} + u_t \end{aligned} \tag{7.21}$$

with the dummy variable defined in (7.18) and $\phi = 1 - \kappa$. For both models, the parameters are estimated simultaneously using nonlinear least squares. To be formal, one can write any of these models in the general form:

$$\begin{aligned} y_t &= f(\mathbf{\Phi}, \mathbf{x_t}) + \xi_t \\ \xi_t &= \phi \xi_{t-1} + u_t \end{aligned} \tag{7.22}$$

The first equation expresses the dependent variable y_t (i.e., the price or the log-price variable) as a function of a vector of parameters, $\mathbf{\Phi}$, and the vector of explanatory variables $\mathbf{x_t}$. The second equation is the first order autoregressive equation of the disturbance term ξ_t in the first equation. Substituting ξ_t in the second equation, and rearranging terms, we get:

$$y_t = \phi y_{t-1} + f(\mathbf{\Phi}, \mathbf{x_t}) - \phi f(\mathbf{\Phi}, \mathbf{x_{t-1}}) + u_t \tag{7.23}$$

whose parameters ϕ and $\mathbf{\Phi}$ are estimated simultaneously using a nonlinear least squares procedure.[13] Finally, we take $\widehat{\kappa} = 1 - \widehat{\phi}$ as the estimate of the mean-reversion parameter κ, and the standard error of the regression as the estimate of σ. Lucia and Schwartz (2005) estimate the coefficients of these models (as well as for two-factor models) using this procedure based on daily electricity prices at the Nordic Power Exchange[14] from January 1, 1993 to December 31, 1999, as provided in Table 7.1.

Table 7.1

	Models based on the Price				Models based on the Log-price			
	Model 1		Model 2		Model 3		Model 4	
Parameter	Estimate	t-statistic	Estimate	t-statistic	Estimate	t-statistic	Estimate	t-statistic
α	153.051	8.146	145.732	8.670	4.938	38.711	4.867	46.192
β	-9.514	-28.085	-9.542	-28.277	-0.090	-28.339	-0.090	-28.523
γ			29.735	2.336			0.306	2.986
τ			6.691	0.269			0.836	0.043
β_2	-2.527	-0.754			-0.027	-0.878		
β_3	-4.511	-0.998			-0.041	-0.977		
β_4	-3.484	-0.664			-0.041	-0.849		
β_5	-13.248	-2.317			-0.185	-3.480		
β_6	-12.656	-2.114			-0.097	-1.744		
β_7	-7.038	-1.157			-0.062	-1.093		
β_8	-8.109	-1.347			-0.101	-1.807		
β_9	-10.061	-1.740			-0.094	-1.749		
β_{10}	-9.597	-1.795			-0.067	-1.352		
β_{11}	-7.304	-1.566			-0.052	-1.190		
β_{12}	-6.019	-1.674			-0.057	-1.703		
ϕ	0.990	355.4	0.989	340.4	0.986	299.0	0.984	277.5
κ	0.010		0.011		0.014		0.016	
S.E. of Regression	9.001		9.222		0.086		0.086	
Adjusted R^2	0.981		0.981		0.974		0.973	
Log likelihood	-9294.2		-9299.0		2652.9		2640.2	
Errors:								
M.A.E.	5.847		5.855		0.053		0.053	
M.A.P.E.	4.980		5.000		1.176		1.179	

Source: Lucia, J. and Schwartz, E. (2001), 32.

Model 1 and model 3 only contain the dummy variable and exclude the cosine cyclical component for the price and log-price, respectively.[15] In the four models, the independent coefficient α is significantly different from zero. The estimates of the coefficients β, ϕ, and σ are virtually indistinguishable between models 1 and 2, and between models 3 and 4. The null hypothesis of $\phi = 1$ is rejected by the usual t-test for every model. This means that the estimate for the reversion coefficient κ, though very small, turns out to be significant in all cases. The coefficient β corresponding to the dummy variable D_t is negative, as expected, and different from zero in the four models, but not all the coefficients of the monthly dummy variables are significant.[16]

Figures 7.3 and 7.4 plot the actual daily system prices against the fitted model estimates, as well as the associated residual errors of equation (7.23), also called the one period-ahead prediction errors.

Two-Factor Model

The one-factor model can be extended to two factors. According to Hillard and Reis (1998), we can model electricity prices based on the two-factor model:

$$\begin{aligned} dS_t &= (r - \delta_t)S_t dt + \sigma_S S_t dW_t^S \\ d\delta_t &= \alpha(\kappa_\delta - \delta_t)dt + \sigma_\delta dW_t^\delta \end{aligned} \tag{7.24}$$

where r is the interest rate, σ_S is the variance of the geometric Brownian motion followed by S, and δ_t is a stochastic convenience yield that follows a mean-reverting process. The variance of the convenience yield represented by σ_δ, α_δ is the speed of adjustment, and

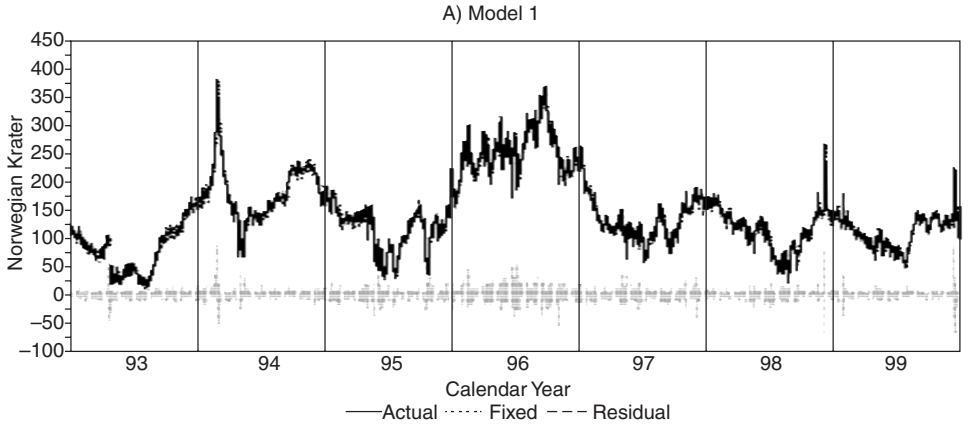

Figure 7.3 *Source: Lucia, J. and Schwartz, E. (2002). Reproduced with permission from Review of Dervatives Research.*

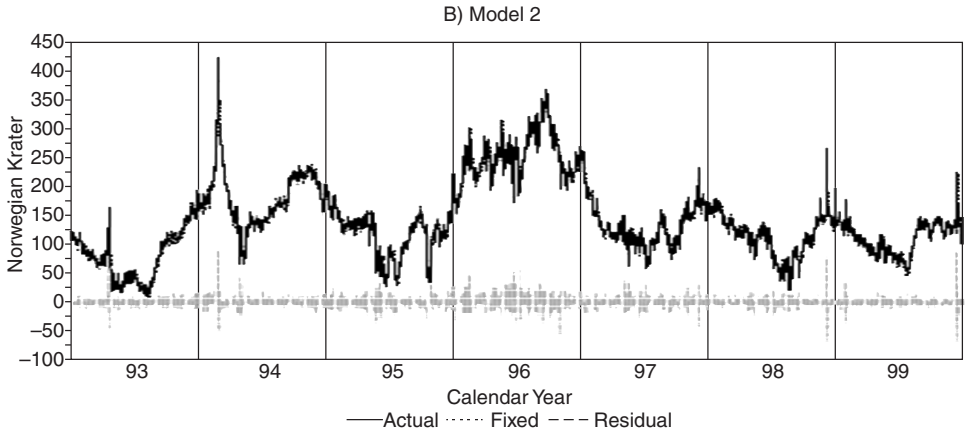

Figure 7.4 *Source: Lucia, J. and Schwartz, E. (2002). Reproduced with permission from Review of Dervatives Research.*

κ_δ is the long-run mean yield. The two Wiener processes W_t^S and W_t^δ are correlated with correlation coefficient ρ. As Doerr (2003) notes, since "the concept of convenience yield is usually only applied to storable commodities, this model is more appropriate for gas or oil prices than electricity."[17] However, it is relevant for swing options, as discussed in the next section. Moreover, the net convenience yield can be "interpreted as a theoretical construction to incorporate the special effects of supply, demand, and other particularities of the power market into one variable."[18] Those effects are "usually stochastic, implying a model for the stochastic behavior of convenience yield. As a key assumption of the model, electricity is therefore modeled as an asset with stochastic (positive or negative) dividend yield δ_t, which itself follows a mean-reverting Ornstein-Uhlenbeck process."[19] We assume that the market price of convenience yield risk is zero.

7.3 Swing Options

In order to hedge market risk arising from sudden changes in the commodity prices, consumers may use forwards or options on the commodity price. However, for some market participants, this reduction of risk is not sufficient because they do not know their exact future need of the commodity. In particular, this is a serious problem with commodities that cannot be stored (e.g., energy and electricity), or for which storage is very expensive. As a result of this problem, so-called swing options have been developed in order to give the holder a certain flexibility with respect to the amount purchased in the future.[20] Because energy is non-storable or expensive to store and exhibits extreme price fluctuations, swing contracts are typically used in the energy markets. This refers specifically to electricity, but swing contracts appear also in coal and gas markets.[21]

We will focus on swing options on electricity. However, the main characteristic properties of swing options—namely, the multiple early exercise features—are the same for all underlying commodities. Typical swing contracts contain a so-called base load agreement (see Jaillet, Ronn, and Tompaidis [2001]). The base load agreement is a set of forward contracts with different expiry dates, t_j, $j = 1, ..., N$. Each forward contract f_j is based on a fixed amount of electricity (or, in general, any commodity), q_j. At each expiry date, the holder has the option to purchase an excess amount or decrease the base load volume.[22] This means that the amount of electricity purchased at a predetermined price (i.e., the strike price) by the holder of the swing option can "swing" within a certain range $(q_j + \Delta_j)$. If Δ_j is positive (negative), the option exercised by the holder at an opportunity time t_j is called upswing (downswing). Thus, an upswing is a buy and a downswing is a sell. For a typical contract, there usually are further restrictions: The total number of upswings, U, and downswings, D, are limited—i.e., $U \leq N$, $D \leq N$, or $U + D \leq N$, for some boundary $N > 0$.

The swing contract might include penalties if the overall volume bought during the term of the contract lies outside the predefined boundaries. These additional constraints lower the price of the swing option on one side. On the other side, they lead to a non-trivial exercise strategy of the option. The reason for this is that the decision to exercise a single swing right does not depend only on the electricity price at that time. Because the number of swing rights are limited, the exercise of one swing right reduces the number of rights available for later exercises. In addition, the exercise (or non-exercise) may result in

penalties. Thus, to exercise a swing right, the payoff from exercise has to exceed the value of the remaining option. As a result, the optimal exercise strategy depends not only on the electricity price, but also on its history and its future distribution.

The combination of swing options with forward contracts is called a swing contract. Swing contracts allow one to add flexibility to the volume of the contract. A typical example for a swing contract is a supply contract. Here, the receiver has the right to receive an arbitrary volume of electricity up to some maximum load. Penalties are introduced in the form of "take-or-pay" clauses, which say that regardless of the volume received, a certain minimum amount of electricity has to be paid in any event. Such a contract can be decomposed into a swing option and a forward contract. The supplier of electricity is selling an implicit swing option.

We will follow the direct work of Doerr (2003) and Meyer (2004) in the discussion that follows on the pricing of swing options.

7.4 The Longstaff-Schwartz Algorithm for American and Bermudan Options

The basic idea of the Longstaff-Schwartz algorithm, described in detail in Longstaff and Schwartz (2001) (and similar approaches like those reported in Clement and Protter (2002)), is to use least squares regression on a finite set of functions as a proxy for conditional expectation estimates. In a first step, the time axis has to be discretized—i.e., if the American option is alive within the time horizon $[0, T]$, early exercise is only allowed at discrete times $0 < t_1 < t_2 < \ldots < t_J = T$. The American option is thus approximated by a Bermudan option. For a particular exercise date t_k, early exercise is performed if the payoff from immediate exercise exceeds the continuation value—i.e., the value of the (remaining) option if it is not exercised at t_k. This continuation value can be expressed as conditional expectation of the option payoff with respect to the risk-neutral pricing measure Q. The expectation is taken conditional on the information set $\Im_{t_k}$, which is available at t_k. Representing the continuation value for a particular sample path ω by $F(\omega, t_k)$, we can write

$$F(\omega, t_k) = E^Q \left[\sum_{j=k+1}^{K} D(t_k, t_j) C(\omega, t_j, t_k, T) | \Im_{t_k} \right] \tag{7.25}$$

where $D(t_k, t_j)$ is the discount factor from t_k to t_j, and $C(\omega, t_j, t_k, T)$ denotes the path of cashflows generated by the option, conditional on the option not being exercised at or prior to time t_k and the holder following the optimal exercise strategy for all remaining opportunities t_j between t_k and T. Note that for every path ω, there is at most one exercise date j where $C(\omega, t_j, t_k, T) > 0$, because Bermudan options have only one exercise right. The decision of exercising at t_{J-1} is made by comparing the continuation value $F(\omega, t_{J-1})$ with the immediate payoff $P(S_{J-1})$, where S_{J-1} is the value of the underlying at time t_{J-1}. While $P(S_{J-1})$ is known, the continuation value has to be estimated.

To find an estimator, the continuation value is represented in a set of basis functions B_j:

$$F(\omega, t_{J-1}) = \sum_{i=0}^{\infty} a_i B_i(S_{J-1})$$

which is approximated by

$$\widehat{F}(\omega, t_{J-1}) = \sum_{i=0}^{M} a_i B_i(S_{J-1}). \tag{7.26}$$

The coefficient a_i is found by regressing the discounted values of $C(\omega, t_J, t_{J-1}, T)$ onto the basis functions. These cashflows are the cashflows that occur at time t_J. The regression is done over all paths that have a continuation value,—i.e., an option is in the money at time t_J. $\widehat{F}(\omega, t_{J-1})$ is an unbiased estimator of the continuation value.

The exercise decision can now be made by comparing the estimator $\widehat{F}(\omega, t_{j-1})$ with the immediate exercise payoff $P(S_{J-1})$ for each path. With the higher of both taken as new cashflow $C(\omega, t_{J-2}, t_{J-1}, T)$ at time t_{J-1}, the iteration is stepped further backward in time.

At the end, the resulting value of the option is calculated by averaging over the cashflows from each path ω:

$$V_{LSM}^{N} = \frac{1}{N} \sum_{i=1}^{N} C(\omega_i) \tag{7.27}$$

Here, $C(\omega_i)$ denotes the discounted cashflow of path ω_i.

The LSM Algorithm

Assume that all interest rates are zero and, therefore, discounting can be omitted. Before starting the actual algorithm, the paths that form the underlying spot prices have to be sampled. For N paths and J exercise opportunities (timesteps), this yields an N x J matrix S, where the matrix $S_{i,j}$ is the spot price in the ith path at time t_j. Next, the set of basis functions $(B_j)_{j=0}^{M}$ for the regression has to be chosen from a great variety of possibilities, including Hermite, Legendre, Chebyshev, Gegenbauer, or Jacobi polynomials.[23] However, Longstaff and Schwartz emphasize that their numerical tests indicate that Fourier or trigonometric series and even simple powers of the state variables also give accurate results. A basis function of order $M = 2$—i.e., quadratic polynomials—works well in the LSM algorithm and is used by Dorr.

$$B_0 = 1$$
$$B_1 = X$$
$$B_2 = X^2$$

The initial step of the actual algorithm is to determine the cashflow vector C^J at the last timestep t_J. These cashflows are easy to get because the continuation values are then zero—i.e.,

$$C_i^J = P(S_{i,J}) \tag{7.28}$$

where P is the payoff function. In the following, we focus on the payoff of a vanilla call option

$$P(S_{i,j}) = \max(S_{i,j} - X_j, 0) \tag{7.29}$$

where the strike prices X_j can vary from timestep to timestep.

Second, we consider the spot prices at timestep t_{J-1} and select those for which $P(S_{i,J-1}) > 0$. This yields the L_{J-1} x 1−vector $\widehat{S}^{J-1}$ where L_{J-1} is the number of in-the-money paths at timestep t_{J-1}. The least squares regression of C^J onto the basis functions B_J is now performed by minimizing the expression

$$\left\| B^{J-1} a^{J-1} - C^J \right\| \tag{7.30}$$

where a^{J-1} is the $(M+1)$ x 1-vector of regression coefficients for timestep t_{J-1} and the matrix B^{J-1} is given by:

$$B^{J-1} = \begin{pmatrix} B_0(\widehat{S}_{1,J-1}) & \dots & B_M(\widehat{S}_{1,J-1}) \\ \vdots & \dots & \vdots \\ B_0(\widehat{S}_{L_{J-1},J-1}) & \dots & B_M(\widehat{S}_{L_{J-1},J-1}) \end{pmatrix} \tag{7.31}$$

The solution of the minimization is given by:

$$a^{J-1} = ((B^{J-1})^T B^{J-1})^{-1} (B^{J-1})^T C^{J-1} \tag{7.32}$$

With that, we obtain the vector of continuation values Cont^{J-1} by:

$$\text{Cont}_i^{J-1} = \sum_{k=0}^{M} a_k^{J-1} B_{i,k}^{J-1} \tag{7.33}$$

Once we have the continuation of values, we perform early exercise whenever

$$P(\widehat{S}_{i,J-1}) > \text{Cont}_i^{J-1}. \tag{7.34}$$

The elements C_i^{J-1} of the cashflow vector C^{J-1} are then given by:

- $P(\widehat{S}_{i,J-1})$, if the early exercise condition (7.34) is true
- 0 otherwise

Subsequently, the elements of the cashflow vector C^J have to be set to zero for those paths where (7.34) is true.

We then step backward through time until we reach the first timestep.[24] At each timestep, early exercise is performed as described previously. Note that whenever a cashflow at timestep t_k is generated by early exercise in path i, all cashflows that occur in this path later than t_k (this is, at most, one) have to be removed.[25]

At the end, we can build the cashflow matrix C from the cashflow vectors C^k by concatenating the cashflow vectors C^k, $k = 1, ..., J$, and the option value is given by the arithmetic average of the row sums.[26]

7.5 Extension of Longstaff-Schwartz to Swing Options

Following the presentation by Doerr,[27] we show how least-squares Monte Carlo can be adopted for the valuation of swing options. Because we now have more than one exercise right, however, we have to deal with an additional "dimension"—i.e., the number of exercises left. Consider a swing option with exercise opportunities at times t_1, t_2, t_3, t_4, and t_5, with five exercise opportunities and three exercise rights (upswings) with a strike price at each opportunity X. Sampling N paths yields N x 5-spot price matrix S. The main difficulties arising from the presence of more than one exercise rights are the following:

- The benefit from immediate exercise is not only the payoff, but the payoff plus the value of the remaining swing option (which has one upswing fewer than the original one).
- When early exercise is performed at time t_k, rearranging the cashflows at later opportunities requires the cashflow matrix of the swing option with one upswing less than the original one.

The generalized cashflow matrix of our algorithm must, therefore, have three dimensions:

- First dimension: number of paths
- Second dimension: number of timesteps (exercise opportunity)
- Third dimension: number of exercise rights (upswings) left

We denote the cashflow matrix for j upswings left as C^j. In our example, there are thus three N x 5 matrices C^1, C^2, and C^3. After the initial step, the cashflow matrices look as follows:

$$C^3 = \begin{pmatrix} \% & \% & P(S_{1,3}) & P(S_{1,4}) & P(S_{1,5}) \\ \% & \% & P(S_{2,3}) & P(S_{2,4}) & P(S_{2,5}) \\ \vdots & \vdots & \vdots & \vdots & \vdots \\ \% & \% & P(S_{N,3}) & P(S_{N,4}) & P(S_{N,5}) \end{pmatrix} \tag{7.35}$$

$$C^2 = \begin{pmatrix} \% & \% & \% & P(S_{1,4}) & P(S_{1,5}) \\ \% & \% & \% & P(S_{2,4}) & P(S_{2,5}) \\ \vdots & \vdots & \vdots & \vdots & \vdots \\ \% & \% & \% & P(S_{N,4}) & P(S_{N,5}) \end{pmatrix} \tag{7.36}$$

$$C^1 = \begin{pmatrix} \% & \% & \% & \% & P(S_{1,5}) \\ \% & \% & \% & \% & P(S_{2,5}) \\ \vdots & \vdots & \vdots & \vdots & \vdots \\ \% & \% & \% & \% & P(S_{N,5}) \end{pmatrix} \tag{7.37}$$

where

$$P(S) = \max(S - X, 0) \tag{7.38}$$

is the payoff of the upswing. The %-signs mean that these cashflows are undefined at this stage. For C^3, we can combine the last three timesteps in the initial step of the algorithm because it is obvious that early exercise takes place at t_3 whenever the payoff at this timestep is positive. Notice that this is the third timestep from the last.

Similarly, when two upswings are left, immediate early exercise is performed at t_4 and thus we can combine the last two timesteps for C^2. The matrix C^1 corresponds to the cashflow matrix in the Longstaff-Schwartz algorithm for Bermudan options. As an example, if we have only six paths, after the initial step, the matrices might look as follows:

$$C^3 = \begin{pmatrix} \% & \% & P_{1,3} & 0 & P_{1,5} \\ \% & \% & P_{2,3} & P_{2,4} & 0 \\ \% & \% & P_{3,3} & 0 & 0 \\ \% & \% & P_{4,3} & P_{4,4} & P_{4,5} \\ \% & \% & P_{5,3} & 0 & P_{5,5} \\ \% & \% & P_{6,3} & P_{6,4} & P_{6,5} \end{pmatrix} \tag{7.39}$$

$$C^2 = \begin{pmatrix} \% & \% & \% & 0 & P_{1,5} \\ \% & \% & \% & P_{2,4} & 0 \\ \% & \% & \% & 0 & 0 \\ \% & \% & \% & P_{4,4} & P_{4,5} \\ \% & \% & \% & 0 & P_{5,5} \\ \% & \% & \% & P_{6,4} & P_{6,5} \end{pmatrix} \tag{7.40}$$

$$C^1 = \begin{pmatrix} \% & \% & \% & \% & P_{1,5} \\ \% & \% & \% & \% & 0 \\ \% & \% & \% & \% & 0 \\ \% & \% & \% & \% & P_{4,5} \\ \% & \% & \% & \% & P_{5,5} \\ \% & \% & \% & \% & P_{6,5} \end{pmatrix} \tag{7.41}$$

Here, all $P_{i,j} = P(S_{i,j})$ are non-zero.

We now start stepping backwards in time. For t_4, we calculate the continuation values for one upswing left by least squares regression of the cashflow vector $\widehat{C}_5^1$ onto the basis functions.[28] In $\widehat{C}_5^1$, only the paths where the payoff at t_4 is positive are considered. We denote the vector of continuation values at timestep four with one upswing left at Cont_4^1.

With the continuation values, we can perform early exercise, and C^1 may look like:

$$C^1 = \begin{pmatrix} \% & \% & \% & 0 & P_{1,5} \\ \% & \% & \% & P_{2,4} & 0 \\ \% & \% & \% & 0 & 0 \\ \% & \% & \% & P_{4,4} & 0 \\ \% & \% & \% & 0 & P_{5,5} \\ \% & \% & \% & P_{6,4} & 0 \end{pmatrix}$$

In our example, early exercise at t_4 was carried out for all possible paths—i.e., paths 2, 4, and 6. Note that for paths 4 and 6, the cashflows at t_5 have been removed. The cashflow matrices C^2 and C^3 remain unchanged in this step.

Now we move on to t_3. In order to get Cont_3^2, we first have to add the cashflow vectors C_4^2 and C_5^2. Denoting the sum vector as C_{4+5}^2, we obtain the relevant sum vector $\widehat{C}_{4+5}^2$ by omitting all paths where $P(S_{i,3})$ is zero. The continuation vector Cont_3^2 is then obtained by linear regression of $\widehat{C}_{4+5}^2$ on the basis functions.

The early exercise condition now reads:

$$P(S_{i,3}) + \text{Cont}_3^1(i) > \text{Cont}_3^2(i) \tag{7.42}$$

That means we have to calculate Cont_3^1 before we can perform early exercise in C^2. This calculation is easily done according to the usual Longstaff-Schwartz algorithm. For those paths where condition (7.42) is fulfilled, early exercise is performed. This means that for each corresponding path, i, $C_3^2(i)$ is set equal to the payoff $P(S_{i,3})$ and the cashflows $C_4^2(i)$ and $C_5^2(i)$ are replaced by $C_4^1(i)$ and $C_5^1(i)$, respectively. After this, early exercise for t_3 is performed in C^1. Although C^3 still remains unchanged in this step, the other cashflow matrices in our example might like the following:

$$C^2 = \begin{pmatrix} \% & \% & P_{1,3} & 0 & P_{1,5} \\ \% & \% & P_{2,3} & P_{2,4} & 0 \\ \% & \% & P_{3,3} & 0 & 0 \\ \% & \% & 0 & P_{4,4} & P_{4,5} \\ \% & \% & 0 & 0 & P_{5,5} \\ \% & \% & P_{6,3} & P_{6,4} & 0 \end{pmatrix} \tag{7.43}$$

$$C^1 = \begin{pmatrix} \% & \% & 0 & 0 & P_{1,5} \\ \% & \% & P_{2,3} & 0 & 0 \\ \% & \% & 0 & 0 & 0 \\ \% & \% & 0 & P_{4,4} & 0 \\ \% & \% & 0 & 0 & P_{5,5} \\ \% & \% & P_{6,3} & 0 & 0 \end{pmatrix} \tag{7.44}$$

For C^2, early exercise was performed in paths 1, 2, 3, and 6. Note that in path 6, the cashflows after t_3 had to be modified according to C^1 at the iteration step before—i.e., t_4. For C^1, early exercise occurs only in paths 2 and 6.

Moving on to t_2, early exercise must be performed for all three cashflow matrices. First, the continuation vectors are calculated by regressing $\widehat{C}_{3+4+5}^J, j = 1, 2, 3$ onto the

basis functions as described previously. Then, early exercise is carried out starting with C^3 by evaluating the condition

$$P(S_{i,2}) + \text{Cont}_2^2(i) > \text{Cont}_2^3(i). \tag{7.45}$$

The condition for C^2 reads

$$P(S_{i,2}) + \text{Cont}_2^1(i) > \text{Cont}_2^2(i). \tag{7.46}$$

For C^1, we obtain

$$P(S_{i,2}) > \text{Cont}_2^1(i). \tag{7.47}$$

Because early exercise includes rearranging the cashflows after t_2 according to the cashflow matrix (with one upswing fewer) at the preceding iteration step, it is important that the procedure is first done with C^3, then with C^2, and finally with C^1. Repeating the same procedure for t_1, we end up with the final cashflow matrices C^1, C^2, and C^3. From these matrices, we obtain the value of the corresponding swing options by taking the average of the row sums.[29]

7.6 General Case: Upswings, Downswings, and Penalty Functions

Application of the LSM algorithm to price swing options must incorporate not only call (upswings), but also put features (downswings). In addition, the algorithm must incorporate penalty functions that depend on the total number of exercises (upswings and downswings).[30] These features have two important implications for the LSM algorithm. First, in the initial step, only the last timestep can be treated because continuation values might be negative because of penalty, and thus it could be sensible to let one or more exercise rights expire worthless. Second, we have an additional dimension—i.e., the number of downswings left.

We introduce some notation:

- u and d are the numbers of upswings and downswings exercised, respectively (in a particular iteration step).
- $u_{\max}$ and $d_{\max}$ are the total numbers of upswings and downswings, respectively.
- J is the number of timesteps (exercise opportunities).

The generalized cashflow tensor has now four dimensions (path, timestep, upswings exercised, and downswings exercised) and consists of $[(u_{\max}+1)\cdot(d_{\max}+1)-1]$ cashflow matrices $C^{u,d}$. Each of these matrices has dimension N *x* J.

In the initial step, we have to evaluate the cashflows at the last exercise opportunities. With $\phi(u,d)$ denoting the penalty function for u upswings and d downswings exercised, we obtain the following cashflows in path i at the final timestep t_J : for $0 \le u < u_{\max}$, $0 \le d < d_{\max}$:

$$C_J^{u,d}(i) = \max[P_u(S_{i,J}) - \phi(u+1,d), P_d(S_{i,J}) - \phi(u,d+1), 0] \tag{7.48}$$

for $0 \leq d < d_{\max}$:

$$C_J^{u_{\max},d}(i) = \max[P_d(S_{i,J}) - \phi(u_{\max}, d+1), 0] \tag{7.49}$$

for $0 \leq u < u_{\max}$:

$$C_J^{u,d_{\max}}(i) = \max[P_u(S_{i,J}) - \phi(u+1, d_{\max}), 0] \tag{7.50}$$

where $P_{u,d}$ is the payoff of the upswing and downswing.

Now starting for a given path, to work backwards from t_J in time, we have to do the following at each step:

- Calculate the continuation values by least squares regression.
- Perform early exercise.

When performing early exercise, we have to step forward from $(u,d) = (0,0)$ to $(u,d) = (u_{\max}, d_{\max})$. It does not matter whether we start with u or d, however. At timestep j (and thus iteration step $J+1-j$), the early exercise conditions for the upswings are for $0 \leq u < u_{\max}$, $0 \leq d < d_{\max}$, $u + d < j$:

$$P_u(S_{i,j}) + \text{Cont}_j^{u+1,d}(i) > \text{Cont}_j^{u,d}(i) \tag{7.51}$$

For the downswings, we obtain for $0 \leq u < u_{\max}$, $0 \leq d < d_{\max}$, $u + d < j$:

$$P_d(S_{i,j}) + \text{Cont}_j^{u,d+1}(i) > \text{Cont}_j^{u,d}(i) \tag{7.52}$$

Eventually, the value of the swing option is obtained by calculating the average of the row sums of $C^{0,0}$ after the final iteration step. Note that in each row, there are at most $u_{\max} + d_{\max}$ non-zero cashflows.

7.7 Swing Option Pricing in Matlab

Refer to Appendix B, "Chapter 7 Code Files," to see the full listing of Matlab code written by Doerr (2004). The code provides the implementation of the LSM algorithm for pricing swing options using upswings, downswings, and penalty functions.

7.8 LSM Simulation Results

Doerr (2003) computes the value of swing options using a one-factor and two-factor mean-reversion model. The follow parameters given in Table 7.2 are used for the one-factor model—see (7.2).

Figure 7.5 shows the swing option value as a function of the spot price for two different values of the mean-reversion speed. The swing consists of 6 upswings and 10 opportunities.

Figure 7.5 shows swing option value as a function of the spot price for two different values of the mean-reversion speed without (left) and with penalty (right). The swing consists of six upswings and four downswings at 10 opportunities. As a consequence of the downswings, the option value exhibits a minimum. Introducing a penalty

Table 7.2

spot value S	20
timesteps	10
time between two timesteps δt	1
exercise rights (upswings)	6
strike at each timestep K	20
mean reversion speed α	0.5
mean reversion level F	20.7387
volatility σ	0.392

Source: Doerr (2004).

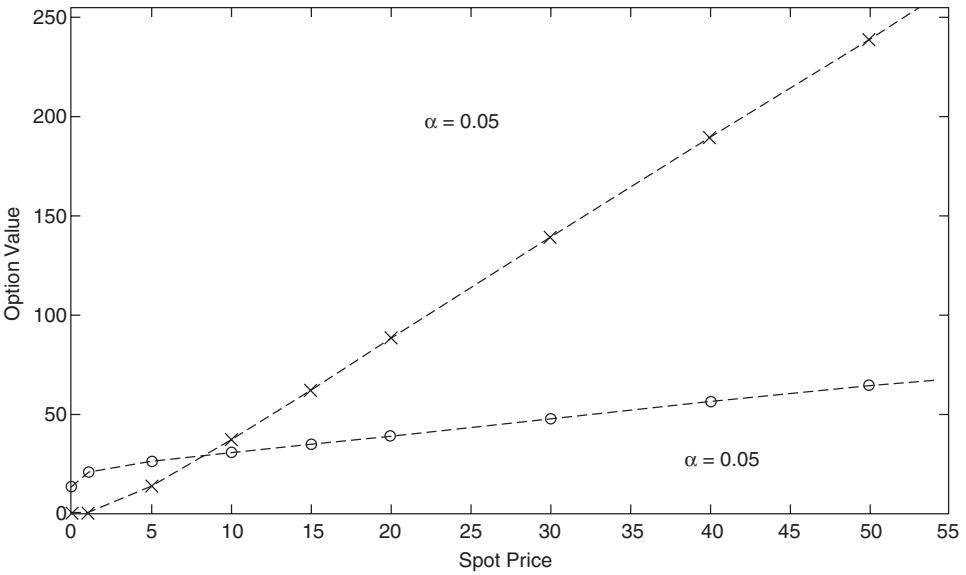

Figure 7.5 *Source: Doerr (2003). Reproduced with permission.*

$$\phi(v) = \begin{cases} 50 & \text{for } v \leq -1 \\ 30(v-2) & \text{for } v > 2 \\ 0 & \text{otherwise} \end{cases}$$

where $v = u - d$ and u and d are the total number of upswings and downswings, respectively, exercised, leads to an overall decrease of the option value, as shown in the left part of Figure 7.6.

The introduction of four downswings in addition to the six upswings (and keeping all other parameters constant[31]) must lead to an overall increase in the swing options value because the new option has more exercise rights while keeping all rights of the old option,[32] as shown in Figure 7.6. Because the downswings are in the money for low spot prices, the option's value as a function of the spot price now exhibits a minimum for both values of α.

Figure 7.7 shows the relative difference between the swing option values obtained by least squares Monte Carlo and finite differences. The calculations have been performed for a swing option with 10 opportunities and mean-reversion speeds of 0.05 (left, no downswings) and 0.5 (right, four downswings). The other parameters are those given in Table 7.2.

The relative deviations are significantly smaller than 1% and thus lie within numerical accuracy. For the Monte Carlo, the accuracy is about 0.3%.

Upper and Lower Boundaries

Because the numerical valuation of Swing options is—in general—quite costly, one tries to find approximation methods that are as simple as possible. In this context, it is important to find upper and lower bounds that can be considered as a first approximation step.

From simple considerations, we can deduce the following boundaries for a swing option with m exercise rights and N opportunities:

- Upper boundary: m Bermudan options (each of them with N opportunities according to the opportunities of the Swing option)
- Lower boundary: Callstrip—i.e., the sum of the m most valuable in the set of the N vanilla call options, which expire at the N opportunities of the Swing option

These boundaries are frequently discussed in the literature about this topic (see Jaillet, Ronn, and Tompaidis [2003], for example) and can be explained in the following way:

- Upper boundary: A holder of m Bermudan options can exercise in the same way a swing option's holder can. Furthermore, he has the right of exercising more than one option at the same opportunity. This means that he has more possibilities than the holder of the swing option, and thus a set of m Bermudan options is an upper boundary for the swing option.
- Lower boundary: The holder of a swing option can exercise at each opportunity, while the holder of the callstrip is restricted to m exercise dates, which are fixed at the beginning. The swing option's holder can exercise at these m dates, but he doesn't

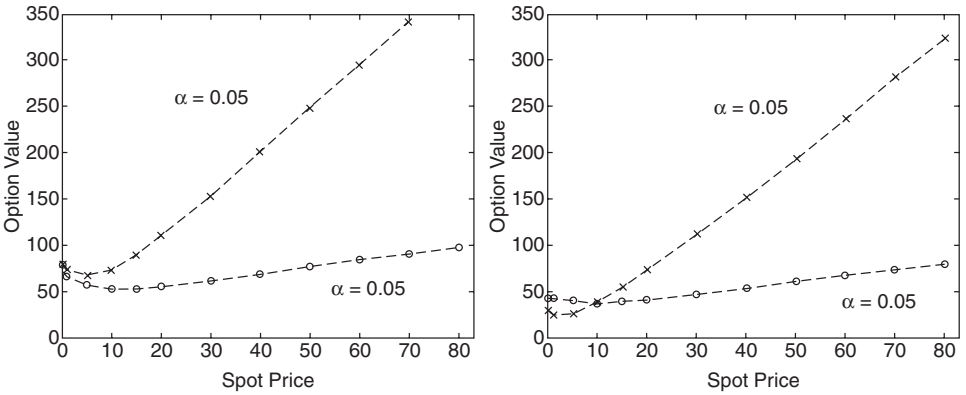

Figure 7.6 *Source: Doerr (2003). Reproduced with permission.*

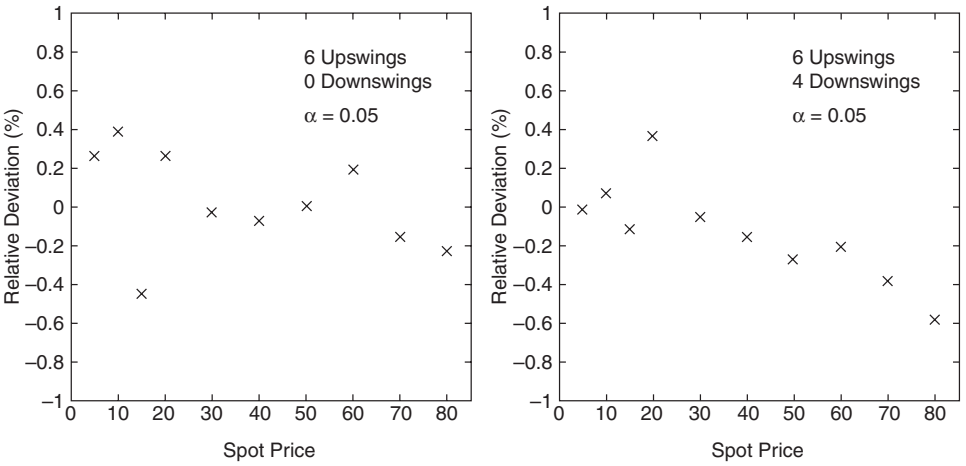

Figure 7.7 *Source: Doerr (2003), 36. Reproduced with permission.*

have to. Thus, the callstrip must be a lower boundary. In the next step, we want to investigate where the swing options value is situated between the two boundaries. We, therefore, introduce the position p:

$$p = \frac{\text{value of Swing option} - \text{lower boundary}}{\text{upper boundary} - \text{lower boundary}}$$

Figure 7.8 shows the empirical error as a function of the number of paths for the two-factor mean-reverting process given in (7.24) with the parameters shown in Table 7.3.

As with the one-factor process, an approximate straight line is given in the logarithmic representation in Figure 7.8.

It is obvious that p lies between 0 and 1. For fixed N, we now consider p as a function of m and immediately find the two trivial cases:

$$p(1) = 1 \tag{7.53}$$

$$p(N) = 0 \tag{7.54}$$

because for $m = 1(N)$, the swing option is the same as the Bermudan option (callstrip). As a computer experiment, $p(m)$ has been determined for both processes and various sets of process parameters.

The line u between the two limiting cases of (7.53) and (7.54) is given by

$$u(m) = \frac{N - m}{N - 1}$$

and the position $u(m)$ corresponds to a swing option value $V_u(m)$ of

$$V_u(m) = \frac{N - m}{N - 1} m \cdot \textit{Bermudan} + \frac{m - 1}{N - 1} \cdot \textit{Callstrip.}$$

Figure 7.9 shows the swing option value as a function of the spot price for the two-factor process. As for the one-factor process, adding downswings leads to an overall increase and the occurrence of a minimum (middle), and subsequent introduction of a penalty leads to an overall decrease of the option value (right).

Exercise Strategies

Doerr (2003) discusses various exercise strategies that impact the valuation of swing options. The valuation of the swing option has been (implicitly) based on the following assumptions:

- The holder applies the optimal exercise strategy.
- The payoff from early exercise can be realized immediately.

However, as Dörr points out, in reality these assumptions are not necessarily fulfilled. First, applying the optimal strategy requires knowledge at each opportunity as to whether it is better to exercise or not. Second, if physical delivery is settled, the holder may not be able to benefit from early exercise because he has to sell the electricity delivered. In this section,

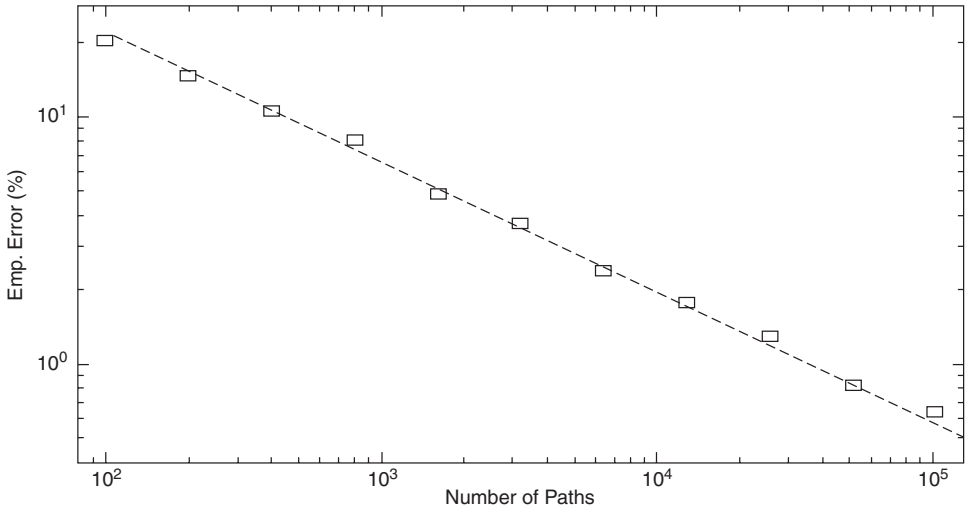

Figure 7.8 *Source: Doerr (2003), pg. 38. Reproduced with permission.*

Table 7.3

spot value S	20
timesteps	6
time between two timesteps δt	1
exercise rights (upswings)	4
strike at each timestep K	20
α	0.5
δ_0	0.05
κ	0.03
σ_S	0.4
σ_δ	0.05
ρ	0.5
r	0.04

Source: Doerr (2003), 36. Reproduced with permission.

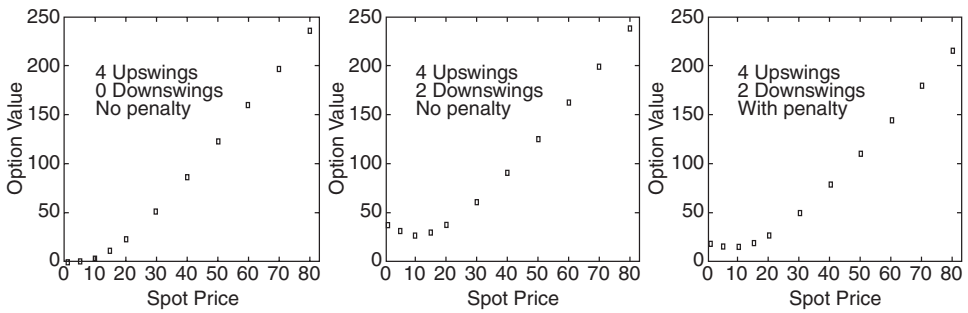

Figure 7.9 *Source: Doerr (2003), pg. 39. Reproduced with permission.*

we focus on the valuation of swing options in terms of different exercise strategies—i.e., we determine the expected payoff under the condition that a particular exercise strategy is applied. In particular, we try to find an approach to the value of a swing option for a holder who

- Does not know the optimal exercise strategy explicitly, or
- Cannot decide by himself when to exercise because he is exposed to external constraints

In the first case, the aim is to find a simple strategy that yields an option value close to the optimal exercise value. This strategy is to be found by simple considerations about the process parameters. An example for the second case could be the following. The holder has bought the swing option in order to protect himself from extremely high spot prices, but he does not know in advance when his need for electricity will occur. When there is no need for electricity, he cannot realize the payoff from an early exercise because he is not able to sell the electricity delivered. Under these circumstances, this holder is interested in knowing the difference between his expected payoff and the market price of the option, which is assumed to be based on optimal exercise. We restrict ourselves to the one-factor (logarithm) process discussed in §7.14. In this way, we keep the number of process parameters small. In particular, this allows us to investigate the interplay of mean-reversion and volatility systematically. Furthermore, some aspects of the early exercise problem can be treated analytically.

The Threshold of Early Exercise

At time t_0, the holder has to decide whether to exercise or not. If the holder decides not to exercise, the option turns into a vanilla call option. Therefore, early exercise is optimal if the payoff from realization is greater than the value of the call option—i.e.,

$$C(S, t_0, t) > S - K$$

where S and K denote the spot and strike prices, respectively. In the following, we keep the strike price K, the mean-reversion level F, and the time to maturity $t - t_0$ constant and consider the value of the vanilla call option as a function of the spot price S, the mean-reversion speed α, and the volatility σ. Omitting the time arguments

$$C(S, \alpha, \sigma) = A(t, t_0)e^{v(t,t_0)/2}N^0_{v(t,t_0)}(d_1) - KN^0_{v(t,t_0)}(d_2) \tag{7.55}$$

where A and v are given by

$$A(t, t_0) = S(t_0)^{e^{-\alpha(t-t_0)}} F^{1-e^{-\alpha(t-t_0)}} \tag{7.56}$$

and

$$v(t, t_0) = \frac{\sigma^2}{2\alpha}(1 - e^{-2\alpha(t-t_0)}). \tag{7.57}$$

With these parameters, d_1 and d_2 can be written as

$$d_1 = \log \frac{A}{K} + v = d_2 + v$$

and $N_b^a(\cdot)$ is the cumulative standard normal distribution defined by

$$N_b^a(\cdot) = \int_{-\infty}^{y} \frac{1}{\sqrt{2\pi b}} e^{-\frac{(x-a)^2}{2b}} dx$$

Differing (7.55) with respect to *S* yields the delta of the call option:

$$\frac{\partial C}{\partial S} = e^{v/2} \frac{\partial A}{\partial S} \left(N_v^0(d_1) + \frac{1}{\sqrt{2\pi v}} e^{-\frac{d_1^2}{2v}} \right) - \frac{K}{A} \frac{\partial A}{\partial S} \frac{1}{\sqrt{2\pi v}} e^{-\frac{d_2^2}{2v}}$$

where

$$\frac{\partial A}{\partial S} = x S^{x-1} F^{1-x}$$
$$x = e^{-\alpha(t-t_0)}$$

Because $0 < x < 1$, we obtain the following limits as $S \to \infty$:

$$A \to \infty$$
$$\frac{\partial A}{\partial S} \to 0$$
$$d_1 \to \infty$$
$$d_2 \to \infty$$

From that, it follows directly that

$$\lim_{S \to \infty} \frac{\partial C}{\partial S} = 0.$$

Figure 7.10 shows a typical plot of a call option against spot price, together with the payoff from immediate exercise. Because both the call and the delta of the call are always greater than zero and delta approaches zero for $S \to \infty$, the equation

$$C(X, t_0, t) = \max(X - K, 0)$$

always has a solution for X—i.e., there is a (unique) threshold for early exercise.

We can show that this threshold is always greater than the mean-reversion level F. This is intuitively clear—why should we exercise early if we know that the spot price is "drawn up" toward F?

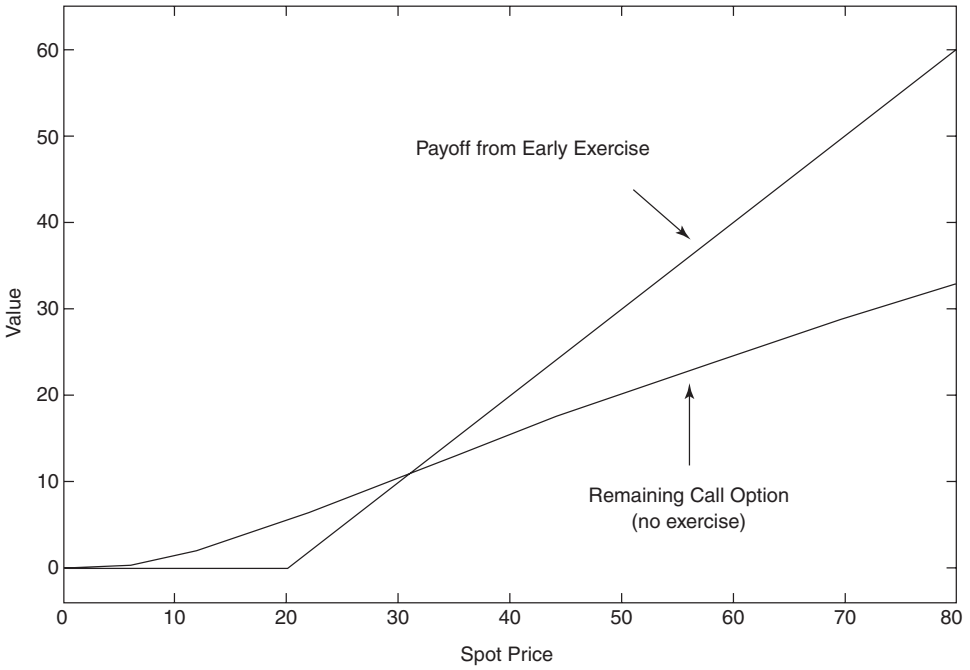

Figure 7.10 *Source: Doerr (2003), 48. Reproduced with permission.*

Doerr (2003) finds that the threshold for early exercise:

- Always exists if $\alpha > 0$
- Is always greater than the mean-reversion level
- Decreases with increasing α and approaches f in the limit $\alpha \to \infty$
- Increases with increasing σ

These results are illustrated in Figure 7.11. Intuitively, it is not surprising that the threshold (which lies always above the mean-reversion level) decreases with increasing mean-reversion speed. If α is large, we should immediately make use of early exercise, because the spot price is expected to be pulled down toward the mean-reversion level. However, if α is large, there is still some hope that the spot price will rise again toward values significantly above the mean-reversion level. Therefore, the need for early exercise is relaxed.

Interplay Between Early Exercise and Option Value

For Bermudan options, the holder can maximize his expected payoff by early exercise. The optimal exercise strategy is very simple: If the spot price at time t_0 exceeds the threshold X, he decides to exercise. However, applying the optimal strategy requires exact knowledge of X. In a simple case, it is quite easy to determine X numerically, but for more

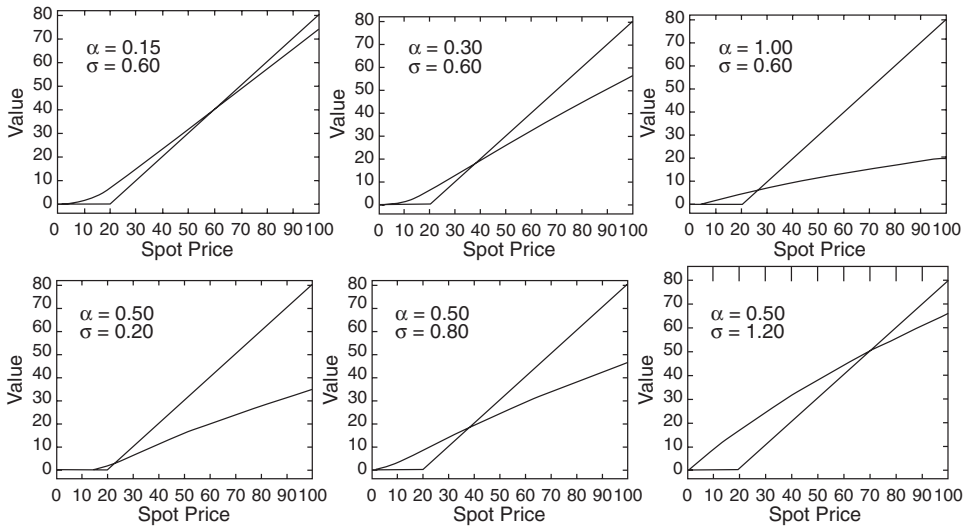

Figure 7.11 *Source: Doerr (2003), 51. Reproduced with permission.*

realistic situations (e.g., more than one opportunity), this may not be the case. Therefore, it is important to investigate the benefit from early exercise in more detail. This means that we should get a feeling for the sensitivity of the expected option payoff to the actual strategy. This shall now be achieved in an intuitive way. As can be seen in Figure 7.11, the cutting angle between the payoff from early exercise and the continuation function increases with increasing α. In Figure 7.12, this is illustrated in an even more drastic manner. For $\alpha = 0.05$, the curves are so close to each other that a suboptimal early exercise decision is expected to have virtually no impact on the expected option payoff. However, the opposite

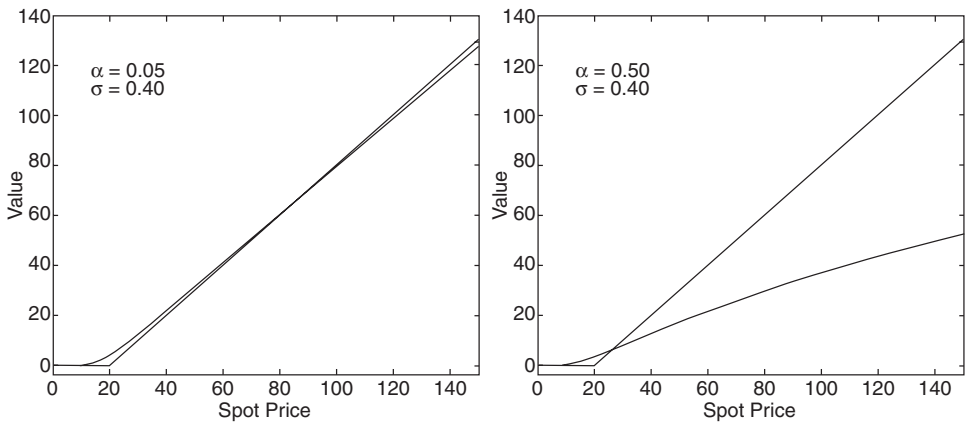

Figure 7.12 *Source: Doerr (2003), 52. Reproduced with permission.*

is right for $\alpha = 0.5$. In this case, the sensitivity of the expected payoff with respect to the actual strategy must be significant.

The cutting angle ϕ is given by:

$$\phi(\alpha, \sigma) = \frac{\pi}{4} - \arctan\left(\frac{\partial C}{\partial S}|_{S=X}\right)$$

We can use ϕ as an indicator for the sensitivity of the expected option payoff on the strategy. For the simple case described previously, it is obvious that the sensitivity increases with increasing ϕ. Because an analytic treatment of ϕ is very difficult (if possible), this has been done numerically. It has turned out that ϕ increases with increasing α, while it decreases with increasing volatility. However, the dependence on α seems to be much stronger than the dependence on σ. See Doerr (2003) for details.

7.9 Pricing of Energy Commodity Derivatives

Cross-Commodity Spread Options

In the petroleum industry, refinery managers are more concerned about the difference between their input and output prices than about the level of prices. Refiners' profits are tied directly to the spread, or difference, between the price of crude oil and the prices of refined products. Because refiners can reliably predict their costs other than crude oil, the spread is their major uncertainty. Crack spread options in crude oil markets, as well as the spark spread and locational spread options in electricity markets, are good examples of cross-commodity derivatives, which play a crucial role in risk management. Spark spread options are derivatives on electricity and the fossil fuels used to generate electricity. Such options are essential in asset valuation for fossil fuel electricity generation plants.[33] A European spark spread call (SSC) option pays a positive part of the difference between the electricity spot price and the generating fuel cost at the time of maturity. Its payoff function is

$$SSC(S_T^e, S_T^g, H, T) = \max\left(S_T^e - H \cdot S_T^g, 0\right) \tag{7.58}$$

where S_T^e and S_T^g are the prices of electricity and the generating fuel, respectively; the constant H is the strike heat price, which represents the number of units of generating fuel contracted to generate one unit of electricity.

A locational spread option pays off the positive part of the price difference between the prices of the underlying commodity at two different delivery points. In the context of electricity markets, locational spread options serve the purposes of hedging the transmission risk and can also be used to value transmission expansion projects[34] (see Deng, Johnson, and Songomonia [1998]). The payoff of a European locational spread call option (LSC) is

$$LSC(S_T^A, S_T^B, L, T) = \max\left(S_T^B - L \cdot S_T^A, 0\right) \tag{7.59}$$

where S_T^a and S_T^b are the commodity prices at locations A and B. The constant L is "a loss factor reflecting the transportation/transmission losses or costs associated with shipping one unit of the commodity from location A to B."[35]

A general cross-commodity spread call option (CSC) is an option with the following payoff at maturity time T:

$$CSC(S_T^1, S_T^2, K, T) = \max\left(S_T^1 - K \cdot S_T^2, 0\right) \tag{7.60}$$

where S_T^i is the spot price of commodity i $(i = 1, 2)$ and K is a scaling constant associated with the spot price of the second commodity. The interpretation of K is different depending on the type of cross-commodity option. For instance, K represents the strike heat rate H in a spark spread option, and it represents the loss factor L in a locational spread option.

The prices of European-type contingent claims on the underlying energy commodity, under various proposed models (discussed later), can be obtained through the inversion of the characteristic transform functions. Suppose $\mathbf{X}_t$ is a state vector in $\Re^n$ and $u \in C^n$. The generalized characteristic transform function is defined as:

$$\begin{aligned}\varphi(u, \mathbf{X}_t, t, T) &= E^Q\left[e^{-r(T-t)} \exp(u \cdot \mathbf{X}_T) | \Im_t\right] \\ &= \exp[A(t,u) + B(t,u)\mathbf{X}_t]\end{aligned}$$

Let $G(v, \mathbf{X}_t, t, T; \mathbf{a}, \mathbf{b})$ denote the time t price of a contingent claim with payoff $\exp(\mathbf{a} \cdot \mathbf{X}_T)$ when $\mathbf{b} \cdot \mathbf{X}_T \leq v$ is true at time T, where $\mathbf{a}$, $\mathbf{b}$ are vectors in $\Re^n$ and $v \in \Re^1$. Then we have:

$$\begin{aligned}G(v, \mathbf{X}_t, t, T; \mathbf{a}, \mathbf{b}) &= E^Q\lfloor e^{-r(T-t)} \exp(\mathbf{a} \cdot \mathbf{X}_t)\, \mathbf{1}_{\mathbf{b}\cdot\mathbf{X}_T \leq v} | \Im_t \rfloor \\ &= \frac{\varphi(\mathbf{a}, \mathbf{X}_t, t, T)}{2} - \frac{1}{\pi}\int_0^\infty \frac{\text{Im}\left\{\varphi(\mathbf{a} + iw\mathbf{b}, \mathbf{X}_t, t, T) e^{-iwv}\right\}}{w} dw\end{aligned}$$

For properly chosen v, $\mathbf{a}$, and $\mathbf{b}$, $G(v, \mathbf{X}_t, t, T; \mathbf{a}, \mathbf{b})$ serves as building blocks in pricing contingent claims such as forwards/futures, call/put options, and cross-commodity spread options.

The value of a European cross-commodity spread call option on two commodities can be found by taking the Fourier transform of (7.58). It can be shown that the price is given by

$$\begin{aligned}CSC(S_t^1, S_t^2, K, t) &= E^Q\lfloor e^{-r(T-t)} \max(S_T^1 - K \cdot S_T^2, 0) | \Im_t \rfloor \\ &= E^Q\lfloor e^{-r(T-t)} \exp(X_T^1) \mathbf{1}_{S_T^1 - K \cdot S_T^2 \geq 0} | \Im_t \rfloor - \\ &\quad K \cdot E^Q\lfloor e^{-r(T-t)} \exp(X_T^2) \mathbf{1}_{S_T^1 - K \cdot S_T^2 \geq 0} | \Im_t \rfloor \\ &= G_1 - K \cdot G_2\end{aligned}$$

where

$$\begin{aligned}G_1 &= G(0, \ln S_t^1, \ln(K \cdot S_t^2), t, T; [1, 0, \cdots, 0]'; [-1, 1, 0, \cdots, 0]') \\ G_2 &= G(0, \ln S_t^1, \ln(K \cdot S_t^2), t, T; [0, 1, \cdots, 0]'; [-1, 1, 0, \cdots, 0]')\end{aligned} \tag{7.61}$$

and

$$G(v, \mathbf{X}_t, t, T; \mathbf{a}, \mathbf{b}) = \frac{\varphi(\mathbf{a}, \mathbf{X}_t, t, T)}{2} - \frac{1}{\pi}\int_0^\infty \frac{\text{Im}\left\{\varphi(\mathbf{a} + iw\mathbf{b}, \mathbf{X}_t, t, T) e^{-iwv}\right\}}{w} dw$$

is the price of the contingent claim at time t and

$$\varphi(u, X_t, Y_t, t, T) = E^Q \lfloor e^{-r(T-t)} \exp\left(u_1 X_T + u_2 Y_T\right) | \Im_t \rfloor$$

is the generalized transform function where $\mathbf{a}$ and $\mathbf{b}$ are vectors in R^n and $v \in R^1$ (see Duffie, Pan, and Singleton [1998] for derivation).

To price energy traded commodity derivatives, Deng (1999) considers three general models: regime-switching, deterministic volatility jump-diffusion, and stochastic volatility jump-diffusion. In each model, the parameters are assumed to be constant, and the jumps appear in the primary commodity price and the volatility processes (Model 3) only. Moreover, the jump sizes are distributed as independent exponential random variables in $\Re^n$, thus having the following transform function:

$$\phi_J^j(\mathbf{c}, t) = \prod_{k=1}^{n} \frac{1}{1 - \mu_j^k c_k} \tag{7.62}$$

where $\mathbf{c}$ is a vector of complex numbers.

Model 1

The jumps are in the logarithm of the primary commodity spot price, X_t. The sizes of type-j jumps ($j = 1, 2$) are exponentially distributed with mean μ_J^j. The transform function of the jump size distribution is $\phi_J^j(c_1, c_2, t) = \frac{1}{1-\mu_J^j c_1}$ for $j = 1, 2$.

$$\begin{aligned} & d\begin{pmatrix} X_t \\ Y_t \end{pmatrix} \\ & \quad = \begin{pmatrix} \kappa_1(\theta_1 - X_t) \\ \kappa_2(\theta_2 - Y_t) \end{pmatrix} dt + \begin{pmatrix} \sigma_1 & 0 \\ \rho_1\sigma_2 & \sqrt{1-\rho_1^2}\sigma_2 \end{pmatrix} dW_t + \sum_{i=1}^{2} \Delta Z_t^i \end{aligned} \tag{7.63}$$

The closed-form solution of the transform function can be written out explicitly for this model as:

$$\varphi_1(u, X_t, Y_t, t, T) = \exp\left(\alpha(\tau) + \beta_1(\tau) X_t + \beta_2(\tau) Y_t\right)$$

where $\tau = T - t$. It can be shown that[36]

$$\begin{aligned} \beta_1(\tau, u_1) &= u_1 e^{-\kappa_1 \tau} \\ \beta_2(\tau, u_1) &= u_2 e^{-\kappa_2 \tau} \\ \alpha(\tau, u) &= -r\tau - \sum_{j=1}^{2} \frac{\lambda_J^j}{\kappa_1} \ln \frac{u_1 u_J^j - 1}{u_1 u_J^j e^{-\kappa_1 \tau} - 1} + \frac{a_1 \sigma_1^2 u_1^2}{4\kappa_1} + \frac{a_2 \sigma_2^2 u_2^2}{4\kappa_2} \\ &\quad + u_1\theta_1(1 - e^{-\kappa_1\tau}) + u_2\theta_2(1 - e^{-\kappa_2\tau}) \\ &\quad + \frac{u_1 u_2 \rho_1 \sigma_1 \sigma_2 (1 - e^{-(\kappa_1+\kappa_2)\tau})}{\kappa_1 + \kappa_2} \end{aligned}$$

with $a_1 = 1 - e^{-2\kappa_1\tau}$ and $a_2 = 1 - e^{-2\kappa_2\tau}$.

Model 2

Model 2 is a regime-switching model with the regime-jumps appearing only in the primary commodity price process. In the electricity markets, this is suitable for modeling the occasional price spikes in the electricity spot prices caused by forced outages of the major power generation plants or line contingency in transmission networks. The model can be used as a joint specification of electricity and the generating fuel price processes under the risk-neutral measure Q. For simplicity, Deng (1999) assumes that there are no jumps within each regime:

$$\begin{aligned} & d\begin{pmatrix} X_t \\ Y_t \end{pmatrix} \\ & \quad = \begin{pmatrix} \kappa_1(\theta_1 - X_t) \\ \kappa_2(\theta_2 - Y_t) \end{pmatrix} dt + \\ & \quad \begin{pmatrix} \sigma_1 & 0 \\ \rho_1\sigma_2 & \sqrt{1-\rho_1^2}\sigma_2 \end{pmatrix} dW_t + v(U_{t^-})dM_t \end{aligned} \tag{7.64}$$

U_t is the regime state process defined as a continuous-time two-state Markov process:

$$dU_t = 1_{U_{t=0}} \cdot \delta(U_t)dN_t^0 + 1_{U_{t=1}} \cdot \delta(U_t)dN_t^1 \tag{7.65}$$

where N_t^i is a Poisson process with arrival intensity λ^i, $i = 0, 1$, and $\delta(0) = -\delta(1) = 1$. M_t is defined as a continuous-time Markov chain:

$$dM_t = -\lambda(U_t)\delta(U_t)dt + dU_t \tag{7.66}$$

and W_t is a standard Brownian motion. $\{v(i) = (v_1(i), v_2(i))', i = 0, 1\}$ denotes the sizes of the random jumps in state variables when regime-switching occurs.

$\phi_{v(i)}(c_1, c_2, t) = \int\limits_{\Re^2} \exp(c \cdot z)dv_{v(i)}(z)$ is the transform function of the regime-jump size distribution $v(i)$, $i = 1, 2$. Z^j, ΔZ^j, and ϕ_J^j are similarly defined as those in Model 1.

The transform function for the model cannot be solved completely in closed-form. We have

$$\begin{aligned} \varphi_2^0(x, y, t) &= \exp\left(\alpha_0(t) + \beta_1(t)x + \beta_2(t)y\right) \\ \varphi_2^1(x, y, t) &= \exp\left(\alpha_0(t) + \beta_1(t)x + \beta_2(t)y\right) \end{aligned}$$

where $\beta(t) = \beta(t, u) = (\beta_1(t, u), \beta_2(t, u))'$ has the closed-form solution of

$$\begin{aligned} \beta_1(\tau, u_1) &= u_1 \exp(-\kappa_1\tau) \\ \beta_2(\tau, u_1) &= u_1 \exp(-\kappa_2\tau). \end{aligned}$$

$\alpha(t) = \alpha(t, u) = (\alpha_0(t, u), \alpha_1(t, u))'$ needs to be numerically computed from

$$\begin{aligned} \frac{d}{dt}\begin{pmatrix} \alpha_0(t) \\ \alpha_1(t) \end{pmatrix} &= -\begin{pmatrix} A_1(\beta(t), t) + \lambda^0\left[\frac{e^{(\alpha_1(t)-\alpha_0(t))}}{1-\mu_0\beta_1(t,u_1)} - 1\right] \\ A_1(\beta(t), t) + \lambda^1\left[\frac{e^{(\alpha_1(t)-\alpha_1(t))}}{1-\mu_1\beta_1(t,u_1)} - 1\right] \end{pmatrix} \\ \begin{pmatrix} \alpha_0(0, u) \\ \alpha_1(0, u) \end{pmatrix} &= \begin{pmatrix} 0 \\ 0 \end{pmatrix} \end{aligned}$$

with

$$A_1(\beta(t),t) = -r + \sum_{i=1}^{2}\left[\kappa_i\theta_i\beta_i + \frac{1}{2}\sigma_i^2\beta_i^2\right] - \rho_1\sigma_1\sigma_2\beta_1\beta_2.$$

Model 3

Model 3 is a stochastic volatility model in which the type-1 jumps are simultaneous jumps in the commodity spot price and volatility processes, and the type-2 jumps are in the commodity spot price only. All parameters are constants.

$$\begin{aligned} d\begin{pmatrix} X_t \\ V_t \\ Y_t \end{pmatrix} &= \begin{pmatrix} \kappa_1(\theta_1 - X_t) \\ \kappa_V(\theta_V - V_t) \\ \kappa_2(\theta_2 - Y_t) \end{pmatrix} dt + \\ &\begin{pmatrix} \sqrt{V_t} & 0 & 0 \\ \rho_1\sigma_2\sqrt{V_t} & \sqrt{(1-\rho_1^2)V_t\sigma^2} & 0 \\ \rho_2\sigma_3\sqrt{V_t} & 0 & \sigma_3 \end{pmatrix} dW_t + \sum_{i=1}^{2}\Delta Z_t^i \end{aligned} \tag{7.67}$$

where W_t is a standard Brownian motion in $\Re^3$. Z^i, $i = 1, 2$, is a compound Poisson process in $\Re^3$. The Poisson arrival intensity functions are $\lambda^1(X_t, V_t, Y_t, t) = \lambda_1$ and $\lambda^2(X_t, V_t, Y_t, t) = \lambda_2 V_t$. The transform functions of the jump-size distributions are

$$\phi_J^1(c_1, c_2, c_3, t) = \frac{1}{(1-\mu_1^1 c_1)(1-\mu_1^2 c_2)}$$

where μ_J^k is the mean size of the type-J ($J = 1, 2$) jump in factor k, $k = 1, 2$. It can be shown that the transform function is of the form (see Deng [1999]):

$$\varphi_3(u, X_t, V_t, Y_t, t, T) = \exp\left(\alpha(t,u) + \beta_1(t,u)X_T + \beta_2(t,u)V_T + \beta_3(t,u)Y_T\right)$$

Deng uses these models to price a spark spread call option with a strike heat rate of $H = 9.5$ MMBtu/Mwh for the previous three models, as well as the geometric Brownian motion (GBM) model. The spark spread call option value converges to the current spot price under the GBM price model. However, under the mean-reversion jump-diffusion price models, it converges to a long-term value, as shown in Figure 7.13, which is most likely to be depending on fundamental characteristics of supply and demand.

Deng uses the model parameter estimates shown in Table 7.4. To estimate the parameters, Deng (1999) derives the moment conditions from the transform function of the unconditional distribution of the underlying price return. Deng assumes that the risk premium associated with the factor X is proportional to X—i.e., the risk premium is of the form $\xi_X \cdot X$. For simplicity, Deng assumes the risk premia associated with the jumps are zero. Deng then uses the electricity and natural gas spot and futures price series to get the estimates for the model parameters under the true measure and the risk premia by matching moment conditions as well as the futures prices.[37]

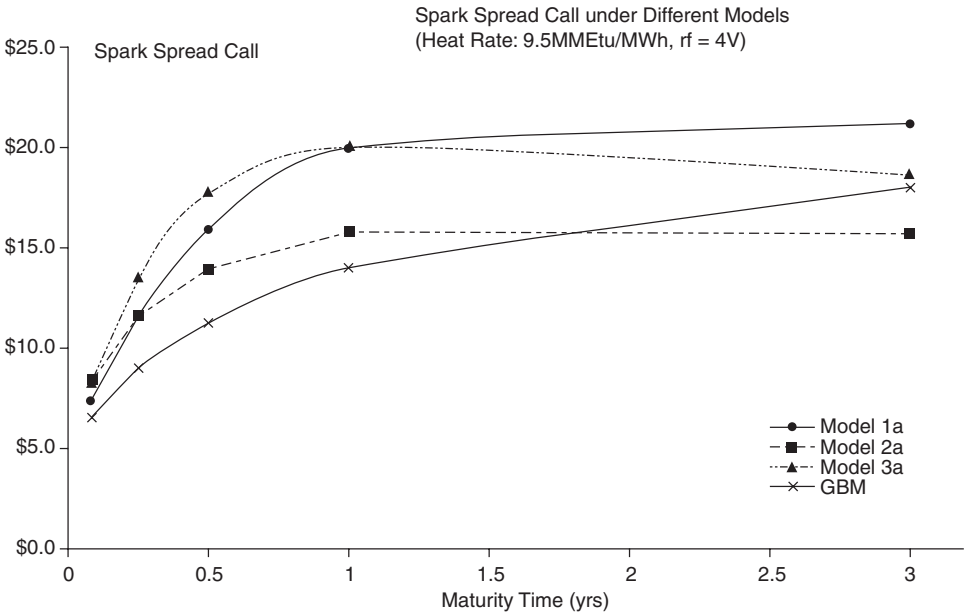

Figure 7.13 *Source: Deng (1999).*

Table 7.4

	Model 1a	Model 2a	Model 3a
κ_1	1.70	1.37	2.17
κ_2	1.80	1.80	3.50
κ_3	N/A	N/A	1.80
θ_1	3.40	3.30	3.20
θ_2	.087	0.87	0.85
θ_3	N/A	N/A	0.87
σ_1	0.74	0.80	N/A
σ_2	0.34	0.34	0.80
σ_3	N/A	N/A	0.54
ρ_1	0.20	0.20	0.25
ρ_2	N/A	N/A	0.20
λ_1	6.08	6.42	6.43
μ_{11}	6.19	0.26	0.23
μ_{12}	N/A	N/A	0.22
λ_2	7.00	8.20	5.00
μ_{21}	-0.11	-0.20	-0.14

Source: Deng (1999).

7.10 JUMP DIFFUSION PRICING MODELS

Various stochastic models have been proposed to capture the mean-reversion and spikes present in electricity prices. The affine jump-diffusion process is a popular choice because they are "flexible enough to capture certain properties such as multiple jumps, time-varying long-term mean, and stochastic volatility in various forms, which occur in many financial time series without sacrificing computational tractability."[38] Following the work of Xiong (2004), we have the models in the next sections.

Model 1a: Affine Mean-Reverting Jump-Diffusion Process

The diffusion part is represented by an Ornstein-Uhlenbeck process, and the jump component has exponentially distributed absolute value of jump size, with the sign of the jump determined by a Bernoulli variable. This is formulated as

$$dX_t = \kappa(\alpha - X_t)dt + \sigma dW_t + J_t dP_t \tag{7.68}$$

where the tuple $\theta = [\kappa, \alpha, \sigma^2, \omega, \psi, \lambda]$ are the unknown parameters. In particular, κ is the mean-reversion rate, α is the long-term mean, W_t is a standard Brownian motion with dW_t $N(0, dt)$ for an infinitesimal time interval dt, and P_t is a discontinuous, one-dimensional standard Poisson process with arrival rate ω. During dt, $dP_t = 1$ if there is a jump, and $dP_t = 0$ otherwise. The jump amplitude J_t is exponentially distributed with mean λ, and the sign of the jump J_t is distributed as a Bernoulli random variable with parameter ψ. It is assumed that the Brownian motion, Poisson process, and random jump amplitude are all Markov and pairwise independent.

The conditional characteristic function (CCF) of X_T, given X_t, $\phi(s, \theta, X_T)|X_t)$, takes the form

$$\begin{aligned}\varphi(s, \theta, X_T|X_t) &= E[\exp(isX_T)|X_t] \\ &= \exp(A(s, t, T, \theta) + B(s, t, T, \theta)X_t)\end{aligned} \tag{7.69}$$

where $A(\cdot)$ and $B(\cdot)$ satisfy the following system of complex-valued ordinary differential equations (ODEs)

$$\begin{aligned}\frac{\partial A(s, t, T, \theta)}{\partial t} &= -\kappa\alpha B(s, t, T, \theta) \\ &\quad - \frac{1}{2}\sigma^2(s, t, T, \theta) - \omega(\varphi(B(s, t, T, \theta)) - 1), \\ \frac{\partial B(s, t, T, \theta)}{\partial t} &= \kappa B(s, t, T, \theta)\end{aligned} \tag{7.70}$$

with boundary conditions

$$A(s, T, T, \theta) = 0, \quad B(s, T, T, \theta) = is. \tag{7.71}$$

Here, the "jump transform" $\varphi(B(s,t,T,\theta)$ is given by:

$$\begin{aligned}\varphi(B(s,t,T,\theta)) &= \psi \int_0^\infty \exp\left(B(s,t,T,\theta)z\right) \frac{1}{\gamma} \exp\left(-\frac{z}{\gamma}\right) dz \\ &\quad + (1-\psi) \int_0^\infty \exp\left(-B(s,t,T,\theta)z\right) \frac{1}{\gamma} \exp\left(-\frac{z}{\gamma}\right) dz \\ &= \frac{\psi}{1 - B(s,t,T,\theta)\gamma} + \frac{1-\psi}{1 + B(s,t,T,\theta)\gamma} \end{aligned} \tag{7.72}$$

Solving (7.69) for $A(\cdot)$ and $B(\cdot)$ and applying the corresponding boundary conditions yields the following:

$$\begin{aligned} A(s,t,T,\theta) &= i\alpha s(1 - e^{-\kappa(T-t)}) - \frac{\sigma^2 s^2}{4\kappa}\left(1 - e^{-2\kappa(T-t)}\right) \\ &\quad + \frac{i\omega(1-2\psi)}{\kappa}\left(\arctan(\gamma s e^{-\kappa(T-t)}) - \arctan(\gamma s)\right) \\ &\quad + \frac{\varpi}{2\kappa} \ln\left(\frac{1 + \gamma^2 s^2 e^{-2\kappa(T-t)}}{1 + \gamma^2 s^2}\right) \\ B(s,t,T,\theta) &= ise^{-\kappa(T-t)} \end{aligned} \tag{7.73}$$

Model 1b

This model allows for asymmetric upward and downward jumps (see Deng [1999], discussed previously), each with exponentially distributed jump magnitudes. The logarithm of the spot price X_t satisfies the SDE

$$dX_t = \kappa(\alpha - X_t)dt + \sigma dW_t + J_t^u dP_t^u(\omega) + J_t^d dP_t^d(\omega) \tag{7.74}$$

where κ is the mean-reversion rate, α is the long-term mean, and W_t is a standard Brownian motion with dW_t $N(0, dt)$. The jump behavior of X_t is governed by two types of jumps: upward jumps and downward jumps. The upward jumps J_t^u are exponentially distributed with positive mean γ_u and jump arrival rate ω_u. The downward jumps J_t^d are also exponentially distributed with negative mean γ_d and jump arrival rate ω_d. Again, P_t^u and P_t^d are two independent discontinuous, one-dimensional standard Poisson processes with arrival rate ω_u and ω_d, respectively.

The transform CCF can be written out as

$$\begin{aligned}\varphi(s,\theta,X_T|X_t) &= E[\exp(isX_T)|X_t] \\ &= \exp(A(s,t,T,\theta) + B(s,t,T,\theta)X_t),\end{aligned}$$

where $A(\cdot)$ and $B(\cdot)$ satisfy the complex-valued system of ODEs:

$$\begin{aligned}\frac{\partial A(s,t,T,\theta)}{\partial t} &= -\kappa\alpha B(s,t,T,\theta) - \frac{1}{2}\sigma^2(s,t,T,\theta) - \omega_u(\varphi_u(B(s,t,T,\theta)) - 1) \\ &\quad - \omega_d(\varphi_d(B(s,t,T,\theta)) - 1) \\ \frac{\partial B(s,t,T,\theta)}{\partial t} &= \kappa B(s,t,T,\theta),\end{aligned} \tag{7.75}$$

with boundary conditions:

$$A(s,T,T,\theta) = 0, \quad B(s,T,T,\theta) = is.$$

Here, the "jump transform" for the upward jump is given by:

$$\begin{aligned}\varphi_u(B(s,t,T,\theta)) &= \int_0^\infty \exp\left(B(s,t,T,\theta)z\right)\left[\frac{1}{\gamma_u}\exp\left(-\frac{z}{\gamma_u}\right)\right]dz \\ &= \frac{1}{1 - B(s,t,T,\theta)\gamma_u}\end{aligned}$$

Similarly, the "jump transform" for the downward jump is given by:

$$\varphi_d(B(s,t,T,\theta)) = \frac{1}{1 - B(s,t,T,\theta)\gamma_d}$$

After some computations, one can solve for $A(\cdot)$ and $B(\cdot)$, applying the boundary conditions:

$$\begin{aligned}A(s,t,T,\theta) &= i\alpha s(1 - e^{-\kappa(T-t)}) - \frac{\sigma^2 s^2}{4\kappa}\left(1 - e^{-2\kappa(T-t)}\right) \\ &\quad + \frac{\omega_u}{\kappa}\ln\left(\frac{1 - is\gamma_u e^{-\kappa(T-t)}}{1 - is\gamma_u}\right) \\ &\quad + \frac{\omega_d}{\kappa}\ln\left(\frac{1 - is\gamma_u e^{-\kappa(T-t)}}{1 - is\gamma_d}\right) \\ B(s,t,T,\theta) &= ise^{-\kappa(T-t)}.\end{aligned} \tag{7.76}$$

Model 2a: Time-Varying Drift Component

Model 1 (7.68) is extended by adding a time-varying component in the drift by replacing the long-term mean α with a deterministic function $\alpha(t)$. The logarithm of the electricity spot price is defined by:

$$dX_t = \kappa(\alpha(t) - X_t)dt + \sigma dW_t + J_t dP_t(\omega) \tag{7.77}$$

The model incorporates on-peak and off-peak effects into the price process by considering the following form for $\alpha(t)$:

$$\alpha(t) = \alpha_1 \text{peak}_t + \alpha_2 \text{offpeak}_t \tag{7.78}$$

where

$$\begin{aligned}\text{peak}_t &= \begin{cases} 1 \text{ if in on-peak periods} \\ 0 \text{ otherwise} \end{cases} \\ \text{offpeak}_t &= \begin{cases} 1 \text{ if in off-peak periods} \\ 0 \text{ otherwise} \end{cases}\end{aligned} \tag{7.79}$$

This is also an affine process. By the same methods, the transform CFF is given by

$$\begin{aligned}\varphi(s,\theta,X_T|X_t) &= E[\exp(isX_T)|X_t] \\ &= \exp(A(s,t,T,\theta) + B(s,t,T,\theta)X_t),\end{aligned}$$

where $A(\cdot)$ and $B(\cdot)$ satisfy the following system of complex-valued ordinary differential equations (ODEs):

$$\begin{aligned}\frac{\partial A(s,t,T,\theta)}{\partial t} &= -\kappa\alpha B(s,t,T,\theta) - \frac{1}{2}\sigma^2(s,t,T,\theta) - \omega(\varphi(B(s,t,T,\theta)) - 1), \\ \frac{\partial B(s,t,T,\theta)}{\partial t} &= \kappa B(s,t,T,\theta),\end{aligned} \tag{7.80}$$

without boundary conditions:

$$A(s,T,T,\theta) = 0, \quad B(s,T,T,\theta) = is.$$

Solving (7.80) for $A(\cdot)$ and $B(\cdot)$ and applying the corresponding boundary conditions yields:

$$\begin{aligned}A(s,t,T,\theta) &= i\alpha s(1 - e^{-\kappa(T-t)}) - \frac{\sigma^2 s^2}{4\kappa}\left(1 - e^{-2\kappa(T-t)}\right) \\ &\quad + \frac{i\omega(1-2\psi)}{\kappa}\left(\arctan(\gamma s e^{-\kappa(T-t)}) - \arctan(\gamma s)\right) \\ &\quad + \frac{\varpi}{2\kappa}\ln\left(\frac{1+\gamma^2 s^2 e^{-2\kappa(T-t)}}{1+\gamma^2 s^2}\right) \\ B(s,t,T,\theta) &= ise^{-\kappa(T-t)}\end{aligned} \tag{7.81}$$

Here, let $t = t_0 < t_1 < \cdots < t_N = T$; then we have

$$\begin{aligned}L(s,t,T,\theta) &= \int_t^T \kappa\alpha(t) ise^{-\kappa(T-t)} dt \\ &= is\sum_{j=1}^{N} \alpha e^{-\kappa(T-t_j)}(1 - e^{-\kappa(t_j - t_{j-1})}),\end{aligned} \tag{7.82}$$

where

$$\alpha = \begin{cases} \alpha_1 & \alpha_1 \text{ if } [t_{j-1}, t_j] \text{ is in on-peak periods} \\ \alpha_2 & \text{otherwise} \end{cases} \tag{7.83}$$

Model 2b: Time-Varying Version of Model 1b

Consider the time-varying extension to Model 1b (7.77), where

$$dX_t = \kappa(\alpha(t) - X_t)dt + \sigma dW_t + J_t^u dP_t^u(\omega) + J_t^d dP_t^d(\omega) \tag{7.84}$$

where $\alpha(t)$ is defined in (7.78).

Similar to the previous models, the transform CCF is of the form

$$\begin{aligned}\varphi(s,\theta,X_T|X_t) &= E[\exp(isX_T)|X_t] \\ &= \exp(A(s,t,T,\theta) + B(s,t,T,\theta)X_t),\end{aligned}$$

where

$$\begin{aligned}A(s,t,T,\theta) &= i\alpha s(1-e^{-\kappa(T-t)}) - \frac{\sigma^2 s^2}{4\kappa}\left(1-e^{-2\kappa(T-t)}\right) \\ &\quad + \frac{\omega_u}{\kappa}\ln\left(\frac{1-is\gamma_u e^{-\kappa(T-t)}}{1-is\gamma_u}\right) \\ &\quad + \frac{\omega_d}{\kappa}\ln\left(\frac{1-is\gamma_u e^{-\kappa(T-t)}}{1-is\gamma_d}\right) \\ B(s,t,T,\theta) &= ise^{-\kappa(T-t)}.\end{aligned} \tag{7.85}$$

with $L(s,t,T,\theta)$ defined in equation (7.82).

7.11 Stochastic Volatility Pricing Models

Jumps alone are inadequate to replicate the level of skewness present in electricity prices. Kaminski (1997) and Deng (1999) emphasize the need to incorporate stochastic volatility in the modeling of electricity spot prices. Volatility in electric prices varies over time and is likely mean-reverting itself (see Goto and Karolyi [2003]). To capture stochastic volatility, various two-factor stochastic volatility models have been proposed by Deng (1999), Xiong (2004), and Villaplana (2002). We consider the two-factor affine process to model electricity spot prices.

Model 3a: Two-Factor Jump-Diffusion Affine Process with Stochastic Volatility

Let X_t be the logarithm of the spot price of electricity and V_t be the volatility of the price process, which evolves stochastically over time.

$$\begin{aligned}d\begin{bmatrix} X_t \\ V_t \end{bmatrix} &= \begin{bmatrix} \kappa(\alpha - X_t) \\ \kappa_v(\alpha_v - V_t) \end{bmatrix} dt \\ &\quad + \begin{bmatrix} \sqrt{(1-\rho^2)V_t} & \rho\sqrt{V_t} \\ 0 & \sigma_v\sqrt{V_t} \end{bmatrix} \begin{bmatrix} dW_t \\ dW_v \end{bmatrix} + \begin{bmatrix} J_t dP_t(\omega) \\ 0 \end{bmatrix}\end{aligned} \tag{7.86}$$

where κ is the mean-reversion rate, α is the long-term mean of the log prices, P_t is a discontinuous, one-dimensional standard Poisson process with arrival rate ω, the amplitude of

J_t is exponentially distributed with mean γ, and the sign of J_t is distributed as a Bernoulli random variable with parameter ψ. The two random variables W_t and W_v are two standard Brownian motions with correlation ρ. Also, κ_v is the mean-reversion rate of the volatility V_t, α_v is the long-term mean of V_t, and σ_v is the volatility of V_t.

Suppose that the jump component in the logarithm of the spot price is defined as in Model 1a and Model 2a. Then, the "jump transform" is given by:

$$\begin{aligned}\varphi\left(\begin{bmatrix} A(\cdot) \\ B(\cdot) \end{bmatrix}\right) &= \int_0^\infty (\psi \exp(A(\cdot)z) + (1-\psi)\exp(-A(\cdot)z)\,\frac{1}{\gamma}\exp\left(-\frac{z}{\gamma}\right) dz \\ &= \frac{\psi}{1-A(\cdot)\gamma} + \frac{1-\psi}{1+A(\cdot)\gamma} \end{aligned} \tag{7.87}$$

The CCF is of the form

$$\begin{aligned}&\varphi(s_x, s_v, \theta, X_T, V_T | X_t, V_t) \\ &\quad = E^\theta[\exp(is_x X_T + is_v V_T)|X_t, V_t] \\ &\quad = \exp(A(s_x, s_v, t, T, \theta)X_t + B(s_x, s_v, t, T, \theta)V_t + C(s_x, s_v, t, T, \theta)),\end{aligned}$$

where $A(\cdot)$, $B(\cdot)$, and $C(\cdot)$ satisfy the following complex-valued Riccati equations:

$$\begin{cases} \frac{\partial A(\cdot)}{\partial t} = \kappa A(\cdot), \\ \frac{\partial B(\cdot)}{\partial t} = \kappa_v B(\cdot) \\ \qquad\qquad -\frac{1}{2}A(\cdot)(A(\cdot) + \rho\sigma_v B(\cdot)) - \frac{1}{2}B(\cdot)(A(\cdot)\rho\sigma_v + B(\cdot)\sigma_v^2) \\ \frac{\partial C(\cdot)}{\partial t} = -\kappa\alpha A(\cdot) - \kappa_v\alpha_v B(\cdot) - \omega(\varphi\left(\begin{bmatrix} A(\cdot) \\ B(\cdot) \end{bmatrix}\right) - 1 \end{cases} \tag{7.88}$$

with boundary conditions:

$$A(s_x, s_v, T, T, \theta) = is_x, \quad B(s_x, s_v, T, T, \theta) = is_v \quad C(s_x, s_v, T, T, \theta) = 0.$$

We can solve the first equation for $A(\cdot)$ and apply the initial conditions to obtain:

$$A(\cdot) = is_x e^{-\kappa(T-t)}$$

However, because there are not closed-form solutions for $B(\cdot)$ and $C(\cdot)$, we need to solve them numerically.

7.12 Model Parameter Estimation

Following the work of Xiong (2004),[39] we discuss how to estimate the parameters of the models. Affine processes are flexible enough to allow us to capture the special characteristics of electricity prices, such as mean-reversion, seasonality, and "spikes." Moreover, under suitable regularity conditions, one can explore the information from the CCF of discretely sampled observations to develop computationally tractable and asymptotically

efficient estimators of the parameters of affine processes. Moreover, the CCF is unique and contains the same information as the conditional density function through the Fourier transform. We can use it to recover the conditional density function via the Fourier transform and implement a usual maximum likelihood (ML) estimation. This is the approach of ML-CCF estimation. If the N-dimensional state variables are all observable, ML-CCF estimation can be implemented, and so obtained ML-CCF estimators are asymptotically efficient (see Singleton [2001]).

The estimation, however, can be costly in higher dimensions $(N \geq 2)$ because we need to compute the multivariate Fourier inversions repeatedly and accurately in order to maximize the likelihood function. According to Singleton (2001), considerable computational saving can be achieved by using limited-information ML-CCF (LML-CFF) estimation (see Singleton [2001]). Suppose $\{\mathbf{X}_t, t = 1, 2, ...\}$ is a set of discretely sampled observations of an N-dimensional state variable with a joint CCF $\phi(s, \theta, \mathbf{X}_{t+1}|\mathbf{X}_t)$. Let η_j denote an N-dimensional selection vector where the jth entry is 1 and zeros elsewhere. Define $X^j_{t+1} = \boldsymbol{\eta}_j \cdot \mathbf{X}_{t+1}$; then the conditional density of X^j_{t+1} conditioned on $\mathbf{X}_t$ is the inverse Fourier transform of $\phi(\xi\boldsymbol{\eta}_j, \theta, \mathbf{X}_{t+1}|\mathbf{X}_t)$ with some scalar ξ:

$$f_j(X^j_{t+1}, \theta|\mathbf{X}_t) = \frac{1}{2\pi} \int_{\Re} \phi(\xi\boldsymbol{\eta}_j, \theta, \mathbf{X}_{t+1}|\mathbf{X}_t) e^{-i\xi\eta_j'\mathbf{X}_{t+1}} ds \tag{7.89}$$

The basic idea behind this is to exploit the information in $f_j(X^j_{t+1}, \theta|\mathbf{X}_t)$ instead of information in the joint conditional density function:

$$f(X_{t+1}, \theta|X_t) = \frac{1}{(2\pi)^N} \int_{\Re^N} \phi(s, \theta, X_{t+1}|X_t) e^{-is'X_{t+1}} ds \tag{7.90}$$

Thus, the estimation involves at most N one-dimensional integrations instead of doing a N-dimensional integration. The estimators obtained are called LML-CCF estimators. Although the LML-CCF estimators do not exploit any information about the joint conditional density function, they are typically more efficient than the quasi-maximum likelihood (QML) estimators for affine diffusions (see Singleton [2001]).

But for those multi-factor models with unobservable (latent) state variables such as stochastic volatility models, the ML-CCF or LML-CCF estimators cannot be obtained. However, several papers discuss the methodologies related to CCF-based estimators of stochastic volatility models. Singleton (1999) proposed a Simulated Method of Moments (SMM-CCF) estimator; Jiang and Knight (1999) explored the Moment of System of Moments (MSM) estimators; Chacko and Viceira (2001) considered the so-called Spectral Generalized Method of Moments (SGMM). SGMM is more computationally tractable than the others (see Singleton [2001]). To deal with stochastic volatility models, Chacko and Viceira (2001) derive stationary (unconditional) characteristic function[40] from the CCF of the volatility, and utilized this CCF to obtain a so-called marginal CCF. An ML type estimation based on the so-called marginal CCF (ML-MCCF) to estimate stochastic volatility models is applied. Furthermore, SGMM estimators based on the so-called marginal CCF to estimate stochastic volatility models are introduced.

ML-CCF Estimators

ML estimation is the most common method of estimating the parameters of stochastic processes if the probability density has an analytical form. It provides a consistent approach to parameter estimation problems, and ML estimators become minimum variance unbiased estimators as the sample size increases. Suppose that $\mathbf{X}$ is an N-dimensional continuous random variable with probability density function $f(\mathbf{X}, \theta)$ where $\theta = \{\theta_1, ..., \theta_k\}$ are k unknown constant parameters that need to be estimated. Given a sequence of observations $\{\mathbf{X}_t\}$ sampled at $t = 1, 2, ..., n$, the log likelihood function at the sample is given by:

$$L(\mathbf{X}_1, ..., \mathbf{X}_n, \theta) = \sum_{t=1}^{n} \ln f(\mathbf{X}_t, \theta) \tag{7.91}$$

The maximum likelihood based estimators of θ are obtained by maximizing $L(\cdot)$

$$\widehat{\theta}_{ml} = \arg\max_{\theta} L(\mathbf{X}_1, \ldots, \mathbf{X}_n, \theta) = \arg\max_{\theta} \sum_{t=1}^{n} \ln(f(\mathbf{X}_t, \theta)). \tag{7.92}$$

For models we adopt, the CCF, $\phi(s, \theta, \mathbf{X}_{t+1}|\mathbf{X}_t)$, of the sample is known, often in closed-form, as an exponential of an affine function of $\mathbf{X}_t$. Thus, the conditional density function of $\mathbf{X}_{t+1}$ given $\mathbf{X}_t$ can be obtained by the Fourier transform of the CCF:

$$f(X_{t+1}, \theta|X_t) = \frac{1}{(2\pi)^N} \int_{\Re^N} \phi(s, \theta, X_{t+1}|X_t) e^{-is' X_{t+1}} ds \tag{7.93}$$

We can use the standard ML estimation based on this conditional density function to obtain ML-CCF estimators of the sample as:

$$\widehat{\theta}_{CCF} = \arg\max_{\theta} \sum_{t=1}^{n} \ln(f(\mathbf{X}_{t+1}, \theta|\mathbf{X}_t)) \tag{7.94}$$

Take Model 1a (7.65) as an example. The conditional density function of $\mathbf{X}_{t+1}$ given $\mathbf{X}_t$ of the sample is of the form:

$$\begin{aligned} f(X_{t+1}, \theta|X_t) &= \frac{1}{2\pi} \int_{-\infty}^{\infty} \phi(s, \theta, X_{t+1}|X_t) e^{-isX_{t+1}} ds \\ &= \frac{1}{2\pi} \int_{-\infty}^{\infty} e^{-isY_t} h(\theta, s) ds, \end{aligned} \tag{7.95}$$

where

$$Y_t = (X_{t+1} - \alpha) - e^{-\kappa}(X_t - \alpha), \tag{7.96}$$

and

$$h(\theta,s)=\exp\left(-\frac{\sigma^2 s^2}{4\kappa}(1-e^{-2\kappa})+\frac{i\omega(1-2\psi)}{\kappa}(\arctan(\gamma s e^{-\kappa})-\arctan(\lambda s)\right)$$
$$+\frac{\omega}{2\kappa}\ln\left(\frac{1+\gamma^2 s^2 e^{-2\kappa}}{1+\gamma^2 s^2}\right) \tag{7.97}$$

To assist in computing this integral (7.95), we define:

$$F(Y_t,\theta)=f(X_{t+1},\theta|X_t)=\frac{1}{2\pi}\lim_{R\to\infty}\int_{-R}^{R}e^{-isY_t}h(\theta,s)ds. \tag{7.98}$$

Notice that $|h(\theta,s)|$ is continuous in s and $|h(\theta,s)|\le-\frac{\sigma^2 s^2}{4\kappa}(1-e^{-2\kappa})$. Thus, we can truncate the integral to finite interval $[-R,R]$ outside of which the function $h(\theta,s)$ to be integrated is negligibly small. Then, for this choice of R,

$$F(Y_t,\theta)\approx\frac{1}{2\pi}\int_{-R}^{R}e^{-isY_t}h(\theta,s)ds. \tag{7.99}$$

Also, we can discretize Y_t into M subintervals such that[41]

$$Y_n=n\Delta Y_t=n\left(\frac{Y_t}{M}\right),$$
$$s_k=k\Delta s=k\left(\frac{R}{M}\right),$$
$$F(Y_t,\theta)\approx\frac{1}{2\pi}\frac{R}{M}\sum_{n=-M}^{M-1\prime}(e^{-ink\frac{RY_t}{M}}h(\theta,\frac{nR}{M})). \tag{7.100}$$

If we arrange $\frac{RY_t}{M}=2\pi$, then we have

$$F(Y_t,\theta)\approx\frac{1}{2\pi}\frac{R}{M}\sum_{n=-M}^{M-1\prime}(e^{-ink\frac{2\pi}{M}}h(\theta,\frac{nR}{M})). \tag{7.101}$$

We can approximate $F(Y_t,\theta)$ by the discrete Fourier transform (DFT) of $h(\theta,\frac{nR}{M})$, and the integral in equation (7.95) can be estimated on a suitable grid of s values by a Fast Fourier transform (FFT) algorithm.

ML-MCCF Estimators

ML-CCF estimators are asymptotically efficient if all of the state variables are observable. But for those multi-factor models with unobservable state variables such as Model 3a and Model 3b, ML-CCF estimators cannot be obtained directly. If option prices are available, implied volatilities can be calculated from option prices observed in the market.

Various numerical methods have been proposed for estimating implied volatility functions from option prices (see Dupire [1994], Coleman, Li, and Verma [1999], and Hamida and Cont [2004]). Then one can use those values as the data of volatilities and implement ML-CCF estimation.

But in our case, option prices are not available. Following Chacko and Viceira (2001), we can integrate the unobservable variable (volatility) from the joint CCF of the log price and the volatility, and set $s_v = 0$, but also need to utilize the volatility information (not workable in our case). Singleton's SMM method integrates out the unobservable variables in the CCF by simulation. This requires a huge number of simulated paths of the volatility and can be quite time-consuming. Furthermore, this induces an estimation bias due to the discretization used in the simulation (see Chacko and Viceira [2001]). Meanwhile, compared to the SGMM method that will be introduced, ML-MCCF estimation avoids the so-called *ad-hoc* moment conditions selection problem and is easier to implement ease of stochastic volatility models.

Take Model 3a as an example. Recall that the volatility follows a square-root process such as

$$dV_t = \kappa_v(\alpha_v - V_t)dt + \sigma_v\sqrt{V_t}dW_v. \tag{7.102}$$

The infinitesimal generator of the square-root process is

$$Lf(v) = \frac{\sigma_v^2 v}{2}\frac{\partial^2 f}{\partial v^2} + \kappa_v(\alpha_v - v)\frac{\partial f}{\partial v}. \tag{7.103}$$

Let μ_t be the distribution function of and then it solves the forward Kolmogorov equation (7.103):

$$\mu_t(Lf) = \frac{d}{dt}\mu_t(f) \tag{7.104}$$

with $\mu_t(f) = \int f(v)d\mu_t$.

In particular, let μ be the stationary characteristic function of the volatility. In this case, with $f(v) = e^{iuv}$ and $\widehat{\mu}(u) = \mu(e^{iuv})$ we have

$$\begin{aligned} Le^{iuv} &= -\frac{\sigma_v^2 v}{2}u^2 e^{iuv} + i\kappa_v(\alpha_v - v)ue^{iuv} \\ &= (iv(\frac{i\sigma_v^2 u^2}{2} - \kappa_v u) + i\kappa_v\alpha_v u)e^{iuv} \end{aligned} \tag{7.105}$$

and

$$\begin{aligned} \mu(Le^{iuv}) &= (\frac{i\sigma_v^2 u^2}{2} - \kappa_v u)\int ive^{ivu}du + i\kappa_v\alpha_v u\int e^{iuv}du \\ &= \left(\frac{i\sigma_v^2 u^2}{2} - \kappa_v u\right)\frac{d\widehat{\mu}(u)}{du} + i\kappa_v\alpha_v u\widehat{\mu}(u) \end{aligned} \tag{7.106}$$

Because $\frac{d\mu(\cdot)}{dt} = 0$, we have

$$\left(\frac{i\sigma_v^2 u^2}{2} - \kappa_v u\right)\frac{d\widehat{\mu}(u)}{du} + i\kappa_v\alpha_v\widehat{\mu}(u) = 0 \tag{7.107}$$

with $\widehat{\mu}(0) = 1$. Then the solution for (7.107) has the form

$$\widehat{\mu} = \left(1 - \frac{iu\sigma_v^2}{s\kappa_v}\right)^{-2\kappa_v\alpha_v/\sigma_v^2}. \tag{7.108}$$

Recall that the joint CCF of the log price and volatility in this model is defined as

$$\begin{aligned}&\phi(s_x, s_v, \theta, X_T, V_T|X_t, V_t)\\ &\quad = \exp\left(A(s_x, s_v, t, T, \theta)X_t + B(s_x, s_v, t, T, \theta)V_t + C(s_x, s_v, t, T, \theta)\right)\end{aligned}$$

where $A(\cdot)$, $B(\cdot)$, and $C(\cdot)$ are the solutions of system (equation (7.88)). As the stochastic volatility V_t is unobservable, we cannot estimate the parameters of stochastic models directly from the joint CCF of the log price and volatility. Let's define the marginal CCF as

$$\begin{aligned}&\phi(s_x, \theta, X_T|X_t)\\ &\quad = \int_0^\infty \phi(s_x, 0, \theta, X_T, V_T|X_t, V_t)d\mu \qquad (7.109)\\ &\quad = e^{A(s_x,0,t,T,\theta)X_t + C(s_x,0,t,T,\theta)} \int_0^\infty e^{B(s_x,0,t,T,\theta)V_t}d\mu\\ &\quad = e^{A(s_x,0,t,T,\theta)X_t + C(s_x,0,t,T,\theta)}\widehat{\mu}(-iB(s_x, 0, t, T, \theta))\end{aligned}$$

Applying equation (7.108), we obtain the marginal CCF of the form

$$\begin{aligned}\phi(s_x, \theta, X_T|X_t) = e^{A(s_x,0,t,T,\theta)X_t + C(s_x,0,t,T,\theta)} \cdot\\ (1 - \frac{B(s_x, 0, t, T, \theta)\sigma_v^2}{2\kappa_v})^{-2\kappa_v\alpha_v/\sigma_v^2}.\end{aligned} \tag{7.110}$$

Through the Fourier transform, the marginal conditional density function is given by

$$f(X_{t+1}, \theta|X_t) = \frac{1}{2\pi}\int_{\Re} \phi(s_x, \theta, X_{t+1}|X_t)e^{-is_xX_{t+1}}ds. \tag{7.111}$$

Then, given a sample $\{X_t, t = 1, ..., n\}$, one can implement the maximum likelihood estimation based on this marginal distribution of the observed variables (electricity prices), and obtain ML-MCCF estimators as

$$\theta_{MCCF} = \arg\max_\theta \sum_{t=1}^{n-1} \ln f(X_{t+1}, \theta|X_t). \tag{7.112}$$

Note that because we only rely on the level of the electricity prices in the previous period, we lose efficiency. And the point estimates (including the SGMM estimators to be discussed), as pointed out by Chacko and Viceira (2001), are biased and inconsistent. In addition, the theoretical value for the bias is hard to calculate as we don't have closed forms

for $B(\cdot)$ and $C(\cdot)$. Following Chacko and Viceira (2001), we try to correct the bias by a bootstrap method. In particular, we simulate 500 paths with a given parameter θ_0. For each path, there are 19,704 hourly observations (same length as the actual data). The estimates $\widehat{\theta}$, $i = 1, ..., n$, obtained from the simulated paths, result in a distribution for each parameter. We will regard the difference between the mean of those estimates and the given parameter as the bias—i.e.,

$$bias = \theta_0 - \frac{1}{n}\sum_{i=1}^{n}\widehat{\theta}_i, \tag{7.113}$$

with $n = 500$ in our setting.[42]

Spectral GMM Estimators

We describe the SGMM estimators constructed by Chacko and Viceira (2001). This method is essentially GMM in a complex variable setting. GMM estimation is one of the most fundamental estimation methods in statistics and econometrics (see Hansen [1982]). Unlike ML estimation, which requires the complete specification of the model and its probability distribution, full knowledge of the specification and strong distributional assumptions are not required for GMM estimation. GMM estimators are best suited to study models that are only partially specified, and they are attractive alternatives to likelihood-type estimators.

Definition 1: Suppose that we have a set of random variables $\{x_t, t = 1, 2, ...\}$. Let $\boldsymbol{\theta} = \theta_1, ..., \theta_k$ be an unknown tuple with true value $\boldsymbol{\theta}_0$ to be estimated; θ_0, θ in some parameter space Θ. Then, the q-dimensional vector of functions $\mathbf{m}(\mathrm{x}_t, \boldsymbol{\theta})$ is called an (unconditional) moment function if the following moment conditions hold:

$$E[\mathbf{m}(x_t, \boldsymbol{\theta}_0)] = \mathbf{0}. \tag{7.114}$$

Notice that θ is a k-tuple vector and $E[\mathbf{m}(x_t, \boldsymbol{\theta}_0)] = \mathbf{0}$ consists of q equations. If we have as many moment conditions as parameters to be estimated $(q = k)$, we can simply solve the k equations in k unknowns to obtain the estimates. If we have fewer moment conditions than unknowns $(q < k)$, then we cannot identify $\boldsymbol{\theta}$. In this case, we can "create" more moment conditions by the so-called weighting functions (often termed "instruments" in the GMM literature; see Matyas [1999]). If we have more functions than unknowns $(q > k)$, then this is an over-identified problem. Such cases of over-identification can easily arise, and the moment estimator is not well-defined. Different choices of moment conditions may lead to different estimates. GMM is a method to solve this kind of over-identification problem.

Consider the standard linear regression model as an example:

$$y = \mathbf{x}'\boldsymbol{\theta}_0 + \varepsilon. \tag{7.115}$$

Here y is the response variable, $\mathbf{x} = [x_1, x_2, \cdots, x_k]'$ is a k-dimensional vector of regressors, $\mathbf{x}'$ is its transpose, and $\boldsymbol{\theta} = [\theta_1, ..., \theta_k]'$ is the unknown vector of parameters

with true value $\boldsymbol{\theta_0}$. We assume that ε has zero expectation and is uncorrelated with $\mathbf{x}$. Using the law of iterated expectations, we find that

$$E[\mathbf{x}\varepsilon] = E[E[\mathbf{x}\varepsilon|\mathbf{x}]] = E[\mathbf{x}E[\varepsilon|\mathbf{x}]] = \mathbf{0}. \tag{7.116}$$

Therefore, we can have the moment functions $\mathbf{m}((\mathbf{x}, y), \boldsymbol{\theta}) = \mathbf{x}(y - \mathbf{x}'\theta)$. These moment functions are well defined, because, by the assumptions

$$E[\mathbf{m}((\mathbf{x}, y), \boldsymbol{\theta}_0)] = E[\mathbf{x}(y - \mathbf{x}'\boldsymbol{\theta}_0)] = E[\mathbf{x}\varepsilon] = 0. \tag{7.117}$$

Suppose $n > k$ observations on the response variable are available—say $y_1, y_2, ..., y_n$. Along with each observed response y_t, we have a k-dimensional observation vector of regressors $\mathbf{x}_t$. We have exactly as many moment conditions as parameters to be estimated, because $\mathbf{x}_t$ is a k-dimensional vector. If we assume that the strong law of large numbers hold, then we have

$$\frac{1}{n}\sum_{t=1}^{n} \mathbf{m}((\mathbf{x}, y), \widehat{\boldsymbol{\theta}}_0) \to E[\mathbf{m}((\mathbf{x}, y), \boldsymbol{\theta}_0] = 0, \text{ almost surely.}$$

So the method of moments (MM) estimator for this model is just the solution of

$$\frac{1}{n}\sum_{t=1}^{n} \mathbf{x_t}(y_t - \mathbf{x_t}'\widehat{\boldsymbol{\theta}}_{\boldsymbol{n}}) = \mathbf{0} \tag{7.118}$$

which gives

$$\widehat{\boldsymbol{\theta}}_{\boldsymbol{n}} = \left(\sum_{t=1}^{n} \mathbf{x_t}\mathbf{x_t}'\right)^{-1} \sum_{t=1}^{n} \mathbf{x_t} y = (\mathbf{X}'\mathbf{X})^{-1}\mathbf{X}'\mathbf{y} \tag{7.119}$$

with $\mathbf{X} = [\mathbf{x_1}, ..., \mathbf{x_n}]$ and $\mathbf{y} = [y_1, ..., y_n]'$. Thus, the ordinary least squares (OLS) estimator is a MM estimator.

Notice that we specified relatively little information about the error term ε. For ML estimation, we would be required to give the distribution of the error term ε, as well as the autocorrelation and heteroskedasticity, which are also not required in formulating the moments conditions.

Now instead of assuming that the error term has zero expectation on certain observed variables, we can specify the moment conditions directly by requiring the error term to be uncorrelated with certain observed "instruments." Let's consider the previous model again. This time, we do not assume the error term has zero expectation, but that it is still uncorrelated to the regressors. Suppose we have a q-dimensional observed instrument $\mathbf{z}$, $(q > k)$ and $E[\mathbf{z}\varepsilon] = \mathbf{0}$. Thus, we have the moment conditions

$$E[\mathbf{z}\varepsilon] = E[\mathbf{z}(y - \mathbf{x}'\boldsymbol{\theta}_0)] = \mathbf{0}, \tag{7.120}$$

and the moment functions

$$\mathbf{m}((\mathbf{x}, y, \mathbf{z}), \theta) = \mathbf{z}(y - \mathbf{x}'\boldsymbol{\theta}). \tag{7.121}$$

If $q = k$, then this is also a well-defined problem. Let $\mathbf{z_t}$ denote the corresponding k-dimensional observation vector of instrument to y_t. We assume that the strong law of large numbers holds, so that we have

$$\frac{1}{n}\sum_{t=1}^{n}\mathbf{m}((\mathbf{x}_t, y, \mathbf{z}_t), \widehat{\boldsymbol{\theta}}_\mathbf{0}) \rightarrow E[\mathbf{m}((\mathbf{x}, y, \mathbf{z})\boldsymbol{\theta}_\mathbf{0}] = \mathbf{0}, \text{ almost surely.} \tag{7.122}$$

Therefore, we solve

$$\frac{1}{n}\sum_{t=1}^{n}\mathbf{z}(y - \mathbf{x}'\widehat{\boldsymbol{\theta}}_\boldsymbol{t}) = \mathbf{0} \tag{7.123}$$

which gives

$$\widehat{\boldsymbol{\theta}}_\boldsymbol{n} = \left(\sum_{t=1}^{n}\mathbf{z_t}\mathbf{x_t}'\right)^{-1}\sum_{t=1}^{n}\mathbf{z_t}y = (\mathbf{Z}'\mathbf{X})^{-1}\mathbf{Z}'\mathbf{y} \tag{7.124}$$

with $\mathbf{Z} = [\mathbf{z}_1, ..., \mathbf{z_n}]$.

The definition of the CCF of sample implied that

$$E[\exp(i\mathbf{s}\cdot\mathbf{X}_T) - \phi(s, \theta, \mathbf{X}_T|\mathbf{X}_t)] = \mathbf{0}, \qquad \mathbf{s} \in \Re^n. \tag{7.125}$$

By taking real and imaginary parts of this function, we get the following pair of moment conditions:

$$\begin{aligned} &E[\text{Re}(\exp(i\mathbf{s}\cdot\mathbf{X}_T) - \phi(s, \theta, \mathbf{X}_T|\mathbf{X}_t))] = \mathbf{0}, \\ &E[\text{Im}(\exp(i\mathbf{s}\cdot\mathbf{X}_T) - \phi(s, \theta, \mathbf{X}_T|\mathbf{X}_t))] = \mathbf{0}. \end{aligned} \tag{7.126}$$

Thus, we can define a set of moment functions

$$\begin{aligned} \mathbf{m}(s, \theta, \mathbf{X}_T, \mathbf{X}_t) &= \varepsilon_t(s, \theta, \mathbf{X}_T, \mathbf{X}_t) = \begin{bmatrix} \varepsilon_t^{\text{Re}}(s, \theta, \mathbf{X}_T, \mathbf{X}_t) \\ \varepsilon_t^{\text{Im}}(s, \theta, \mathbf{X}_T, \mathbf{X}_t) \end{bmatrix}, \\ \varepsilon_t^{\text{Re}}(s, \boldsymbol{\theta}, \mathbf{X}_T, \mathbf{X}_t) &= \text{Re}(\varepsilon_t(s, \boldsymbol{\theta}, \mathbf{X}_T, \mathbf{X}_t)) = \text{Re}(\exp(i\mathbf{s}\cdot\mathbf{X}_T) - \phi(s, \boldsymbol{\theta}, \mathbf{X}_T|\mathbf{X}_t)), \\ \varepsilon_t^{\text{Im}}(s, \boldsymbol{\theta}, \mathbf{X}_T, \mathbf{X}_t) &= \text{Im}(\varepsilon_t(s, \boldsymbol{\theta}, \mathbf{X}_T, \mathbf{X}_t)) = \text{Im}(\exp(i\mathbf{s}\cdot\mathbf{X}_T) - \phi(s, \boldsymbol{\theta}, \mathbf{X}_T|\mathbf{X}_t)). \end{aligned}$$

More generally, we can add a set of "instruments" or "weighting functions" to obtain more restrictions. So we can define the moment function based on the CCF as[43]

$$\mathbf{m}(s, \theta, \mathbf{X}_T, \mathbf{X}_t) = \boldsymbol{\varepsilon}_t(s, \theta, \mathbf{X}_T, \mathbf{X}_t) \otimes \mathbf{p}(\mathbf{X}_t),$$

where $\mathbf{p}(\mathbf{X}_t)$ are "instruments" independent of $\boldsymbol{\varepsilon}_t(s, \theta, \mathbf{X}_T, \mathbf{X}_t)$ and $\otimes$ is the Kronecker product. The SGMM estimator is of the form:

$$\widehat{\boldsymbol{\theta}}_{\mathbf{SGMM}} = \arg\min_{\boldsymbol{\theta}}\left[\frac{1}{n}\sum_{t=1}^{n}\mathbf{m}(s, \boldsymbol{\theta}, \mathbf{X}_T, \mathbf{X}_t)\right]' \mathbf{W_n}\left[\frac{1}{n}\sum_{t=1}^{n}\mathbf{m}(s, \boldsymbol{\theta}, \mathbf{X}_T, \mathbf{X}_t)\right],$$
$$\theta \in \Theta.$$

Just as for other GMM estimators, the asymptotic variance of the SGMM estimator is minimized with the optimal weighting matrix $W_n = S^{-1}$, where S is the covariance matrix of the moment functions (see Chacko and Viceira [2001]). Under the usual regularity conditions, according to Chacko and Viceira (2001), the SGMM estimator, $\widehat{\boldsymbol{\theta}}_{\mathbf{SGMM}}$, inherits the optimality properties of GMM estimators such as consistency and asymptotic normality (see Hansen [1982]).

We can now apply SGMM to estimate stochastic volatility models like Model 3a and Model 3b. Recall that the marginal CCF of the sample is given by

$$\begin{aligned}&\phi(s_x, \theta, X_{t+1}|X_t)\\ &\quad = e^{A(s_x,0,t,\theta)X_t + C(s_x,0,t,\theta)}(1 - \frac{B(s_x,0,t,\theta)\sigma_v^2}{2\kappa_v})^{-2\kappa_v\alpha_v/\sigma_v^2}\end{aligned} \tag{7.127}$$

where $A(\cdot)$, $B(\cdot)$, and $C(\cdot)$ are the solutions of system (7.88) for Model 3a and Model 3b, respectively. Given a sample $\{X_t, t = 1, ..., T\}$, we have moment functions as follows:

$$\begin{aligned}\mathbf{m}(s_x, X_t, \theta) &= \varepsilon_t(s_x, X_t, \theta) = \begin{bmatrix} \varepsilon_t^{\text{Re}}(s_x, X_t, \theta) \\ \varepsilon_t^{\text{Im}}(s_x, X_t, \theta) \end{bmatrix}, \\ \varepsilon_t^{\text{Re}}(s_x, X_t, \theta) &= (\cos(s_x X_{t+1}) - \text{Re}(\phi(s_x, 0, X_{t+1}|X_t))) \otimes \mathbf{p}(X_t), \\ \varepsilon_t^{\text{Im}}(s_x, X_t, \theta) &= (\sin(s_x X_{t+1}) - \text{Im}(\phi(s_x, 0, X_{t+1}|X_t))) \otimes \mathbf{p}(X_t).\end{aligned} \tag{7.128}$$

with $\phi(s_x, 0, X_{t+1}|X_t)$ defined as equation (7.127). Following Chacko and Viceira (2001), we can compute the n-th conditional moment by simple substitution $s_x = n$ into equation (7.128).

In order to construct the moment functions, Xiong (2004) uses the first six spectral moments by setting $s_x = 1, 2, ..., 6$ and $\mathbf{p}(X_t)$ as a T-dimensional vector of 1s. The estimates are biased and inconsistent (see Matyas [1999]). Using this methodology, Xiong finds the parameter estimates for Model 3a, shown in Table 7.5.

Table 7.5

	Estimate	Std.	T-ratio
κ	0.1152	0.0023	50.0870
α	-0.5086	0.0413	-12.3148
ω	1.0814	0.0170	63.6118
ψ	0.5781	0.0090	64.2333
γ	0.3522	0.0065	54.1846
ρ	-0.9710	0.0014	-693.5714
κ_{ϖ}	0.5483	0.0315	17.4063
α_{ϖ}	0.0261	0.0020	13.0500
σ_{ϖ}	0.1529	0.0171	8.9415
Log-likelihood	-11345.8013		

Source: Xiong (2004).

Simulation

Figure 7.14 shows the peak electricity prices (EP) superimposed by simulation paths for Model 1b. The plot also includes a sample plot of peak electricity prices, one typical simulated path, the 95% quantile, and 5% quantile of the simulation.

Figure 7.15 shows the offpeak EP superimposed by simulation paths for Model 1b. The plot also includes a sample plot of peak electricity prices, one typical simulated path, the 95% quantile, and 5% quantile of the simulation.

Figures 7.16 and 7.17 show a comparison of simulated price processes with Peak EP (Model 1b) and offpeak EP (Model 1b), respectively Note that the histogram in Figure 7.16 is of the change of the deseasonalized peak EP, and the histogram in Figure 7.17 is of the change of the deseasonalized offpeak EP. The overlaid black line is the corresponding distribution of the log returns of one typical simulated path. Note that this model underestimates the number of small changes and overestimates the medium-sized changes.

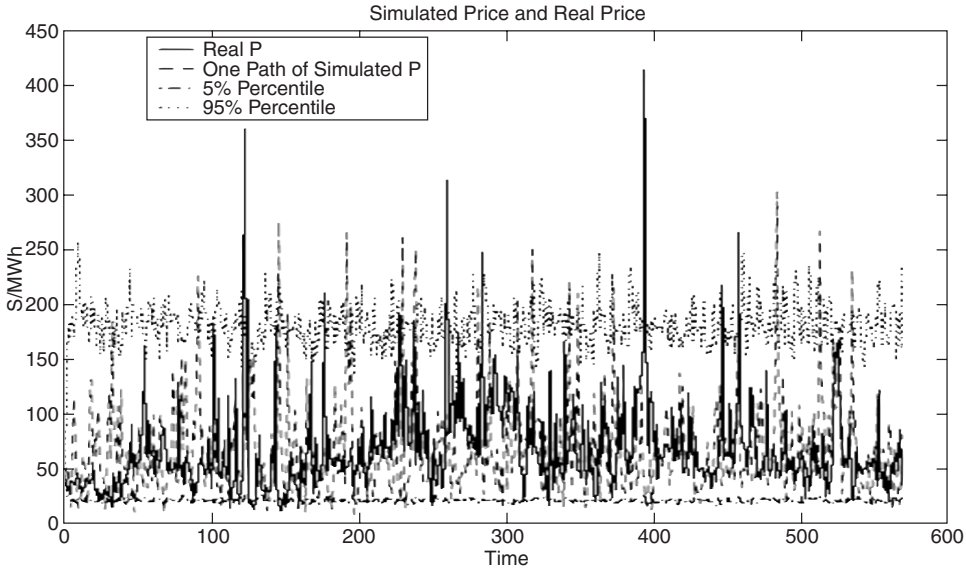

Figure 7.14 *Source: Xiong (2004). Reproduced with permission.*

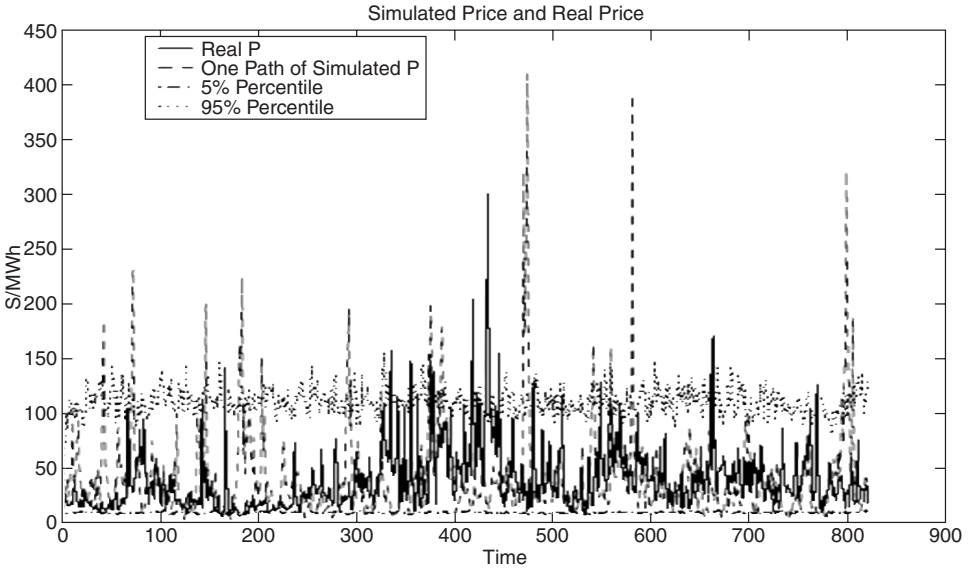

Figure 7.15 *Source: Xiong (2004). Reproduced with permission.*

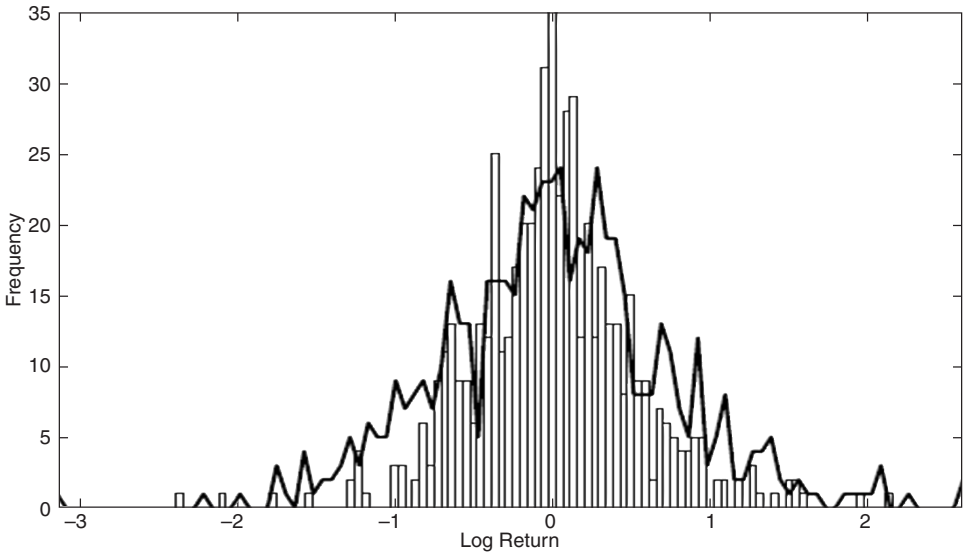

Figure 7.16 *Source: Xiong (2004). Reproduced with permission.*

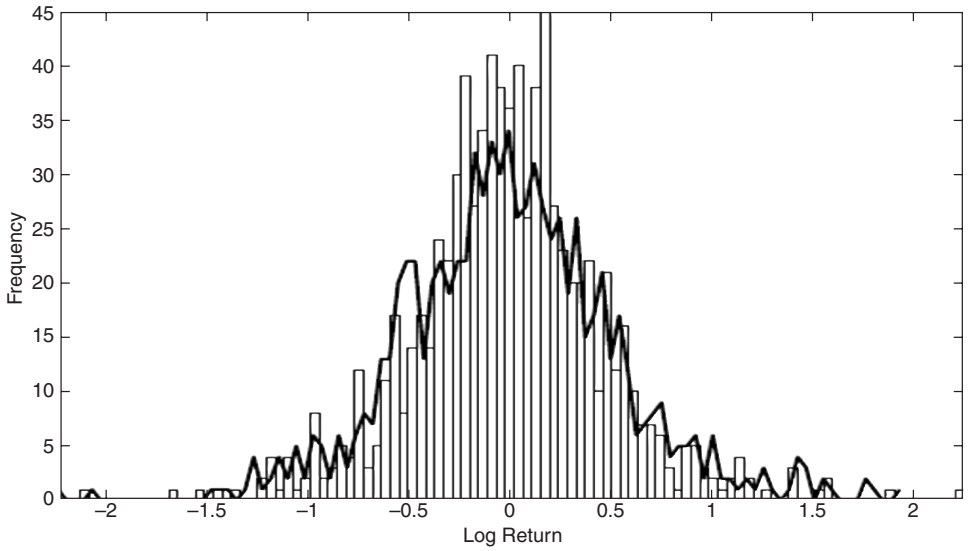

Figure 7.17 *Source: Xiong (2004). Reproduced with permission.*

7.13 Parameter Estimation in Matlab

Refer to Appendix B to see the full listing of the Matlab code, written by Lei Xiong and Anthony Ware, that estimates the model parameters using the maximum likelihood methodology from Xiong (2004) given in the previous section. The market data Xiong and Ware used to calibrate and estimate the model parameters (stored in the array and used in the functions) is from the Alberta Nordic Pool (but not provided).

7.14 Energy Commodity Models

A common mean-reverting model used to model energy commodity prices for instruments like the crack spread contract[44] is the Schwartz-Ross model:

$$dS_t = \alpha(L - \ln S_t)S_t dt + \sigma S_t dW_t \tag{7.129}$$

where W_t is a standard Brownian motion, and α, L, and σ are all positive constant numbers. In this model, S_t mean reverts to the long-term mean $\widehat{L} = e^L$. Applying Ito's lemma for $X_t = \ln S_t$, we have

$$dX_t = \alpha(L - \frac{\sigma^2}{2\alpha} - X_t)dt + \sigma dW_t \tag{7.130}$$

which is an Ornstein-Uhlenbeck process. Rather than reversion to the long-term mean of the logarithm of the price, reversion to the price level itself can be modeled by the Dixit-Pinkyck model:

$$dS_t = \alpha(L - S_t)S_t dt + \sigma S_t dW_t \tag{7.131}$$

where W_t is a standard Brownian motion, and α, L, and σ are all positive constant numbers. Each of these parameters could be made time-varying and stochastic.

In contrast to other types of commodity prices like sugar and gold, energy commodity prices show no discernable trends. As shown in Figure 7.18, spot prices for crude oil (West Texas Intermediate at Cushing, Oklahoma), heating oil (New York Harbor), unleaded gasoline (New York Harbor), and natural gas (Henry Hub, LA) appear to fluctuate randomly.

Heating oil and gasoline prices tend to move with the crude oil prices, while spot markets of natural gas (discussed in the next section) peak periodically with no obvious warning. In general, energy commodities also have higher volatility than other types of commodities. Electricity commodities have the highest volatility, while financial commodities have the lowest, as shown in Figure 7.19, which displays the average annual historical spot market price volatility for various commodities from 1992 to 2001.

We can use these volatility estimates for σ in models (7.129) to (7.131).

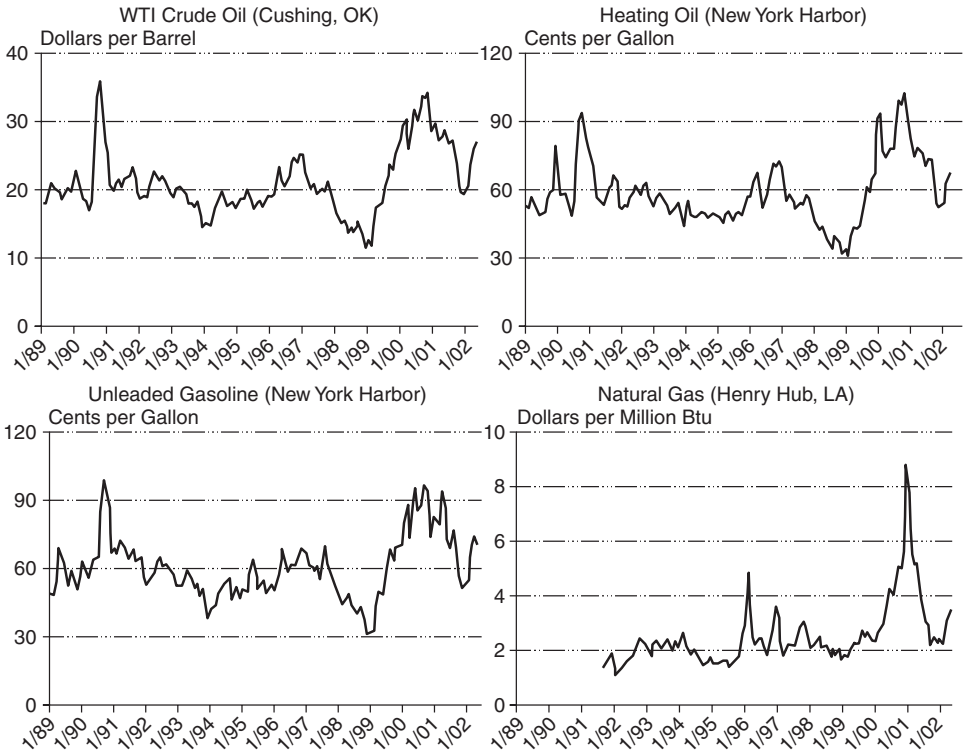

Figure 7.18 *Source: Commodity Futures Trading Commission (see Energy Information Administration/Derivatives and Risk Management in Energy Industries, U.S. Dept. of Energy, (2002), pg. 10).*

Commodity	Average Annual Volatility (Percent)	Market	Period
Electricity			
California-Oregon Border	309.9	Spot-Peak	1996-2001
Cinergy	435.7	Spot-Peak	1996-2001
Palo Verde	304.5	Spot-Peak	1996-2001
PJM	389.1	Spot-Peak	1996-2001
Natural Gas and Petroleum			
Light Sweet Crude Oil, LLS	38.3	Spot	1989-2001
Motor Gasoline, NYH	39.1	Spot	1989-2001
Heating Oil, NYH	38.5	Spot	1989-2001
Natural Gas	78.0	Spot	1992-2001
Financial			
Federal Funds Rate	85.7	Spot	1989-2001
Stock Index, S&P 500	15.1	Spot	1989-2001
Treasury Bonds, 30 Year	12.6	Spot	1989-2001
Metals			
Copper, LME Grade A	32.3	Spot	January 1989-August 2001
Gold Bar, Handy & Harman, NY	12.0	Spot	1989-2001
Silver Bar, Handy & Harman, NY	20.2	Spot	January 1989-August 2001
Platinum, Producers	22.6	Spot	January 1989-August 2001
Agriculture			
Coffee, BH OM Arabic	37.3	Spot	January 1989-August 2001
Sugar, World Spot	99.0	Spot	January 1989-August 2001
Corn, N. Illinois River	37.7	Spot	1994-2001
Soybeans, N. Illinois River	23.8	Spot	1994-2001
Cotton, East TX & OK	76.2	Spot	January 1989-August 2001
FCOJ, Florida Citrus Mutual	20.3	Spot	September 1998-December 2001
Meat			
Cattle, Amarillo	13.3	Spot	January 1989-August 2001
Pork Bellies	71.8	Spot	January 1989-August 2001

Figure 7.19 *Source: Energy Information Administration/Derivatives and Risk Management in the Energy Industries, U.S. Dept. of Energy (2002).*

7.15 NATURAL GAS

Natural Gas Markets

Natural gas is an important energy resource that consumers often demand and use as a cheaper alternative to other energy resources like electricity. The main use of natural gas[45] is in heating, power generation, as a household fuel, and as a chemical feedstock. Natural gas accounts for about a quarter of total energy consumption in North America. The deregulation of the natural gas industry in North America with the enactment of the American Natural Gas Policy Act of 1978 has led to a dynamic, highly competitive market with fluctuating prices. Before price deregulation, the market for domestic oil and gas derivatives was limited. Under price regulation, the U.S. Department of Energy (DOE), the Federal Energy Regulatory Commission (FERC), and the State public utility commissions (PUCs) directly or indirectly controlled the prices of domestic crude oil, petroleum products, wellhead natural gas, pipeline transmission, and retail gas service.

As a result of this deregulated environment, market participants like natural gas producers found themselves exposed to volatile price movements and to counterparty performance risk, which led to a substantial increase in the need for risk management. This in turn, led to the development of spot and forward markets in natural gas. As a result, the New York Mercantile Exchange (NYMEX) launched the world's first natural gas futures contract in April 1990. Since then, gas futures contracts have been widely used to hedge against price fluctuations in this volatile market. The standardization of contract terms, relatively small contract size, fungibility, lack of requirement of physical delivery, and rigorous performance requirements attracted many market participants like natural gas producers, marketers, processors, utilities, and end users, as well as speculators. Volume and open interest have grown rapidly establishing the gas contract as the fastest-growing instrument in NYMEX history. In 2002, the daily average volume of NYMEX market exceeded 97,000 contracts, which involves several times the average daily consumption of gas in North America. Figure 7.20 shows the major pricing points (hubs) for natural gas in the U.S. The Henry Hub in Louisiana is one the major hubs.

World trade in natural gas is divided among major regional markets dominated by pipeline infrastructures that provide the means of transporting the gas from producers to consumers and a single worldwide market for liquefied natural gas (LNG). The United States is the largest pipeline gas market. In 2000, the United States produced 19.3 trillion cubic feet of natural gas and consumed 23 trillion cubic feet. The supply gap was covered

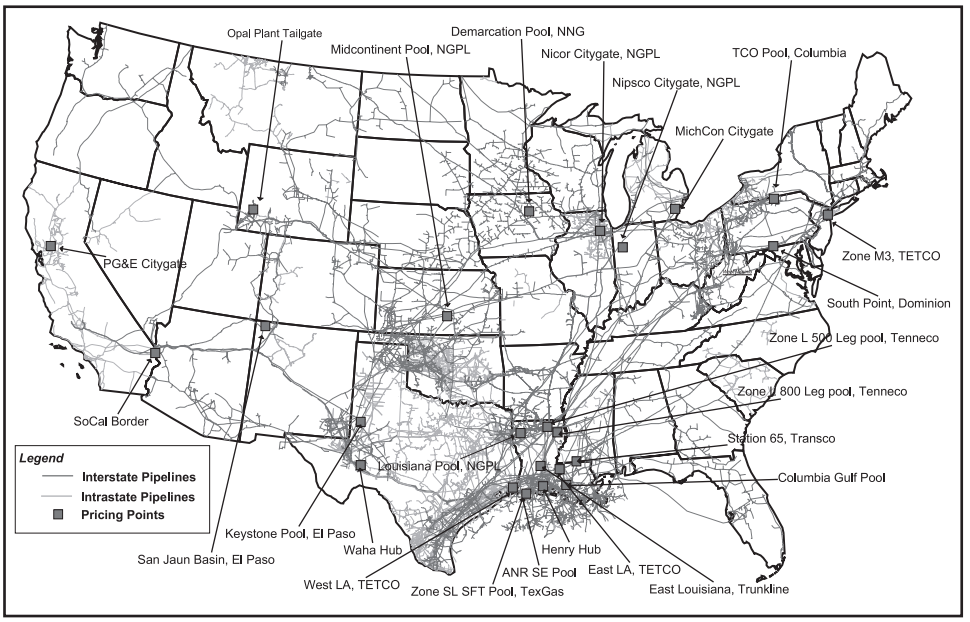

Source: Energy Information Administration, EIAGIS-NG Geographic Information System.

Figure 7.20 *Source: Energy Information Administration/ Derivatives and Risk Management in Energy Industries, U.S. Department of Energy (2002), pg. 19.*

by 3.2 trillion cubic feet of imports from Canada and 0.5 trillion cubic feet of LNG from the world market. The European countries produced 10.5 trillion cubic feet and consumed 16.2 trillion cubic feet, with the supply gap covered by Russian imports and small amounts of imported LNG. Russia was the world's largest producer of natural gas in 2000 at 20.3 trillion cubic feet, followed by the United States and Canada. Major exporters of LNG are Indonesia, Malaysia, Australia, Qatar, Oman, Nigeria, and Trinidad. Japan is the largest importer of LNG.

Natural gas, like electricity, is a network industry in the sense that all suppliers and users are linked by the physical distribution system for the commodity. Pipelines have no effective competition for moving gas within the United States. Figure 7.20 shows the general locations served by major pipelines and several of the spot markets (pricing points) that have emerged at major trans-shipment points (hubs).

Location arbitrage does not work as well for natural gas and electricity as it does for crude oil. Because gas pipelines and power lines have essentially no competitors, frustrated customers cannot buy supplies "off system." In addition, it is difficult to achieve competitive transmission pricing. Consequently, transmission charges are set in noncompetitive markets, with the result that arbitrary price differences between and across markets, not based on marginal costs, can persist in more or less independent, local markets.

Natural Gas Spot Prices

There are a number of fundamental factors that drive complex gas price behavior, including extraction, storage, transport, weather, policies, technological advances, and so on. Figure 7.21 illustrates the plot of daily gas spot prices, which are measured in dollars per million British thermal units (MMBTU), at the Henry Hub in Louisiana, one of the largest hubs in the U.S., from January 2, 1992 to December 30, 1999.

There are several important properties associated with the behavior of gas spot prices. Like electricity prices, gas prices exhibit mean-reversion. In addition, while prices move up and down frequently, they actually oscillate around an equilibrium level from the point of long-term view, which is the effect of mean-reversion.[46] The mean-reversion in natural gas appears to be correlated with the reaction of the market to events such as floods, summer heat waves, and other news-making events, which can create new and unexpected supply-and-demand imbalances in the market. A correction to either the supply side, to match the demand side, or the actual dissipation of the event, such as the temperatures reverting to their average seasonal levels, tends to cause the natural gas prices to come back to their average levels.[47] The speed of mean-reversion depends on how quickly it takes for supply and demand to return to a balanced state or for the events to dissipate. The long-term mean around which the prices oscillate is determined by the cost of production and the normal level of demand.[48]

Seasonality is also an important property of gas prices. Seasonality results primarily from regular demand fluctuations, which are driven by recurring weather-related factors. As we know, natural gas is a primary residential and commercial space heating fuel and is used increasingly as a fuel for electricity generation. The cold winter weather results in above-average consumption of natural gas, while in some hot summers, demand increases for power generation to run air conditioning and other cooling devices.[49] On the other hand,

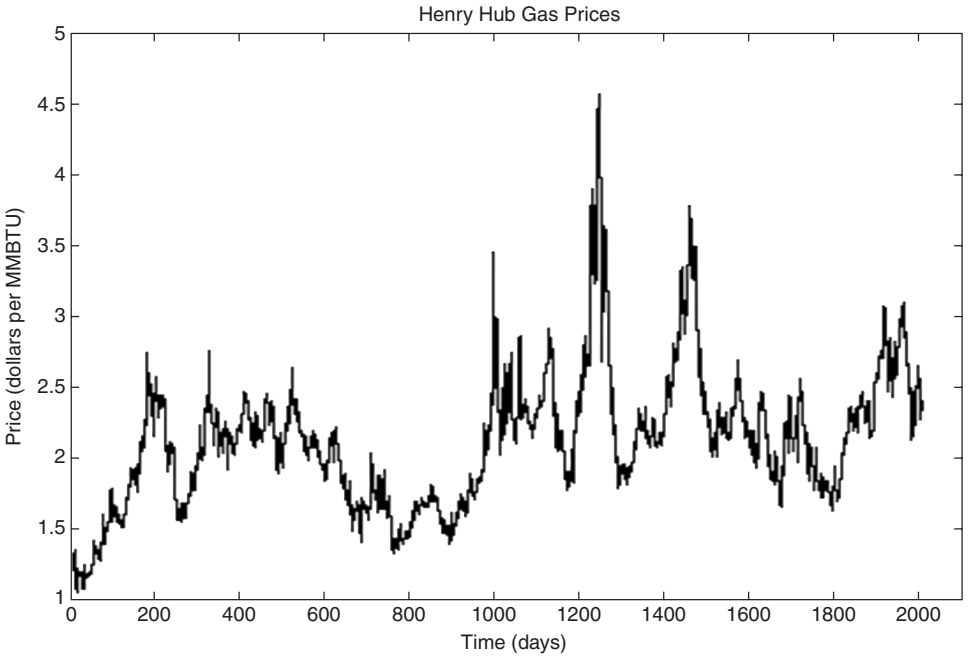

Figure 7.21 *Source: Xu (2004). Reproduced with permission.*

"the difficulty of storage and the limitation of transmission capacity make the supply side not elastic enough to match the suddenly increased demand side very quickly."[50]

7.16 Gas Pricing Models

We can model gas prices similar to electricity prices. Consider gas spot prices as the sum of a seasonal term $f(t)$ and an unseasonalized state term X_t, where X_t follows a one-factor mean reverting process with constant long-term mean and time-dependent volatility.

One-Factor Model

Following Xu (2004), let

$$S_t = f(t) + X_t \tag{7.132}$$

where

$$f(t) = bt + \sum_{i=1}^{N} \beta_i \cos\left(\frac{2\pi i t}{365}\right) + \nu_i \sin\left(\frac{2\pi i t}{365}\right) \tag{7.133}$$

and

$$dX_t = \alpha(L - X_t)dt + \sigma(t)X_t^r dW_t \tag{7.134}$$

where

$$\sigma(t) = \exp\left(c + \sum_{j=1}^{K} \lambda_j \cos\left(\frac{2\pi it}{365}\right) + \omega_j \sin\left(\frac{2\pi jt}{365}\right)\right)$$

where W_t is a Brownian motion, $r = 0$, $\frac{1}{2}$, or 1, and $b, \beta_i's$, $v_i's$, $\alpha, L, c, \lambda_j's$, and $\omega_i's$ are all constant. The volatility term $\sigma(t)$ is of an exponential form in order to ensure that it is positive. The linear term bt in $f(t)$ contributes to capture the tendency of the prices. The sine and cosine function in $f(t)$ and $\sigma(t)$ make them move up and down periodically as seasons change. Furthermore, the trigonometric functions corresponding to $N = 1$ and $K = 1$ capture the annual seasonality, because the period of these functions is 365, the number of days in the year; the trigonometric functions corresponding to $N = 2$ and $K = 2$ capture the semiannual seasonality, because the period of these functions is half a year.

Using Henry Hub prices from January 2, 1992 to December 30, 1999, Xu (2004) estimates the parameters of the one-factor model without seasonality using maximum likelihood estimation, as shown in Table 7.6.

Table 7.6

	Model 1	Model 2
	$r = 0$	$r = 1/2$
α	0.0181	0.0139
L	2.1441	2.1526
σ	0.0870	0.0549

Source: Xu (2004).

Two-Factor Model

Consider a system of SDEs describing these models:

$$\begin{cases} dS_t = \alpha(L_t - S_t)dt + \sigma S_t^r dW_t^1 \\ dL_t = \mu(\gamma - L_t)dt + \tau L_t^r dW_t^2 \end{cases} \tag{7.135}$$

where α, σ, μ, γ, and τ are constant and $r = 0$, $\frac{1}{2}$, or 1. We assume that the Wiener processes dW_t^1 and dW_t^2 are uncorrelated. In this two-factor model, the natural gas spot price long-term mean is a random variable that follows its own mean-reverting process rather than geometric Brownian motion. Seasonality can be incorporated into this model. The gas spot price can be viewed as the sum of a seasonal term $f(t)$ and an unseasonalized state term X_t, which follows a two-factor mean-reverting process.

Mathematically, let

$$S_t = f(t) + X_t$$

where

$$f(t) = bt + \sum_{i=1}^{N} \beta_i \cos\left(\frac{2\pi it}{365}\right) + \eta_i \sin\left(\frac{2\pi it}{365}\right)$$

and X_t follows a mean-reverting process described by

$$\begin{cases} dS_t = \alpha(L_t - S_t)dt + \sigma(t)S_t^r dW_t^1 \\ dL_t = \mu(\gamma - L_t)dt + \tau L_t^r dW_t^2 \end{cases}$$

where

$$\sigma(t) = \exp\left(c + \sum_{j=1}^{K} \lambda_j \cos\left(\frac{2\pi i t}{365}\right) + \omega_j \sin\left(\frac{2\pi j t}{365}\right)\right).$$

In the preceding equations, W_t^i's are Wiener processes, $r = 0$, $\frac{1}{2}$, or 1, and b, β_i's, η_i's, α, μ, γ, τ, c, λ_j's, and ω_j's are all constant, while N and K are positive integers.

To price futures contracts on natural gas, we take the expectation of (7.135) under the risk-neutral measure:

$$\begin{cases} dS_t = \widetilde{\alpha}(L_t - S_t)dt + \sigma\sqrt{S_t}dW_t^1 \\ dL_t = \widetilde{\mu}(\gamma - L_t)dt + \tau\sqrt{L_t}dW_t^2 \end{cases}$$

where $\widetilde{\alpha}$, $\widetilde{\mu}$, and $\widetilde{\gamma}$ are the risk-neutral parameters, and we assume a square root process $(r = 1/2)$. We then find that

$$\begin{cases} d\bar{S}_t = \widetilde{\alpha}(\bar{L}_t - \bar{S}_t)dt \\ d\bar{L}_t = \widetilde{\mu}(\widetilde{\gamma} - \bar{L}_t)dt \end{cases} \tag{7.136}$$

where $\bar{S}_t$ and $\bar{L}_t$ are the expectation values of S_t and L_t at time t respectively. Solving the second ODE for $\bar{L}_t$ with boundary condition that at $t = t_0$, $\bar{L}_t = L_{t_0}$, we obtain:

$$\bar{L}_t = (L_{t_0} - \widetilde{\gamma})e^{\widetilde{\mu}(t_0 - t)} + \widetilde{\gamma} \tag{7.137}$$

Plugging in (7.136) into the first ODE in (7.135) for $\bar{S}$, with the boundary condition that at $t = t_0$, $\bar{S}_t = S_{t_0}$, we obtain that

$$\begin{aligned} \bar{S}_t &= S_{t_0}e^{\widetilde{\alpha}(t_0 - t)} + \frac{\widetilde{\alpha}}{\widetilde{\alpha} - \widetilde{\mu}}(L_{t_0} - \widetilde{\gamma})(e^{\widetilde{\mu}(t_0 - t)} - e^{\widetilde{\alpha}(t_0 - t)}) - \widetilde{\gamma}(1 - e^{\widetilde{\alpha}(t_0 - t)}) \\ &= e^{\widetilde{\alpha}(t - T)}S_{t_0} + \frac{\widetilde{\alpha}}{\widetilde{\alpha} - \widetilde{\mu}}(e^{\widetilde{\mu}(t_0 - t)} - e^{\widetilde{\alpha}(t_0 - t)})L_{t_0} + \frac{\widetilde{\mu}\widetilde{\gamma}}{\widetilde{\alpha} - \widetilde{\mu}}(e^{\widetilde{\mu}(t_0 - t)} - 1) - \\ &\quad \frac{\widetilde{\mu}\widetilde{\gamma}}{\widetilde{\alpha} - \widetilde{\mu}}(e^{\widetilde{\mu}(t_0 - t)} - 1). \end{aligned}$$

Because $F^{\tilde{\theta}}(t, T, S_t) = \bar{S}_t$, and at initial time $t_0 = t$, $\bar{S}_{t_0} = S_t$, and $\bar{L}_{t_0} = L_{t_0}$, the gas futures price under the risk-neutral measure is

$$\begin{aligned} &F^{\tilde{\theta}}(t, T, S_t) \\ &\quad e^{\widetilde{\alpha}(t - T)}S_t + \frac{\widetilde{\alpha}}{\widetilde{\alpha} - \widetilde{\mu}}(e^{\widetilde{\mu}(t - T)} - e\widetilde{\alpha}(t - T)L_t + \\ &\quad \frac{\widetilde{\mu}\widetilde{\gamma}}{\widetilde{\alpha} - \widetilde{\mu}}(e^{\widetilde{\mu}(t - T)} - 1) - \frac{\widetilde{\mu}\widetilde{\gamma}}{\widetilde{\alpha} - \widetilde{\mu}}(e^{\widetilde{\mu}(t - T)} - 1). \end{aligned} \tag{7.138}$$

If seasonality is included, then the futures price is

$$F^{\widetilde{\theta}}(t,T,S_t) = f(T) + e^{\widetilde{\alpha}(t-T)}(S_t - f(t)) + \frac{\widetilde{\alpha}}{\widetilde{\alpha}-\widetilde{\mu}}(e^{\widetilde{\mu}(t-T)} - e\widetilde{\alpha}(t-T)L_t + \frac{\widetilde{\mu}\widetilde{\gamma}}{\widetilde{\alpha}-\widetilde{\mu}}(e^{\widetilde{\mu}(t-T)}-1) - \frac{\widetilde{\mu}\widetilde{\gamma}}{\widetilde{\alpha}-\widetilde{\mu}}(e^{\widetilde{\mu}(t-T)}-1). \tag{7.139}$$

Calibration

To calibrate and estimate the parameters of the model, maximum likelihood estimation can be used. *Calibration* is essentially a process of matching the information observed from the market so that the better the information matched, the more accurate the calibration. Seasonality can be inferred from the natural gas spot prices and futures prices. To reveal the seasonal term $f(t)$, a natural idea is to exploit the information in both spot and futures prices.

One-Factor Model Calibration

Denote the historical spot prices by $\{S_t\}_{t=1}^n$, and the futures prices by $\{F_{t,T_{ii}}|t = 1,2,...,n; i = 1,2,...,m\}$, where T_{ti} is the ith delivery after t, and m is the number of futures prices that we can observe at time t. These are the data we can obtain from the real market. On the other hand, under the assumption that the spot price follows the process described by equations (7.132)–(7.134), we have the theoretical futures price function $F^{\widetilde{\theta}}(t,T,S_t)$ for a one-factor model with seasonality given by

$$F^{\widetilde{\theta}}(t,T,S_t) = e^{\widetilde{\alpha}(t-T)}(S_t - \widetilde{L} - f(t)) + \widetilde{L} + f(T) \tag{7.140}$$

where t is the observing time, T is the delivery time, and $\widetilde{\theta}$ is the set of active parameters—i.e., $[b, \beta_1, \beta_2, ..., \beta_N, \eta_1, \eta_2, ..., \eta_N, \widetilde{\alpha}, \widetilde{L}]$.

To match the real market data to the model, we need to find some appropriate parameters to make the theoretical futures prices and the actual futures prices as close as possible. If the distance between two vectors is defined in Euclidean space, then the estimation of $\widetilde{\theta}$ can be obtained by minimizing the sum of the squares of the differences between $F^{\widetilde{Q}}(t,T_{ti},S_t)$ and $F_{t,T_{ii}}$, for $t = 1,2,...,n; i = 1,2,...,m$. In particular, we need to solve:

$$\widetilde{\theta} = \arg\min_{\widetilde{\theta}} \sum_{t=1}^{n}\sum_{i=1}^{n}(F^{\widetilde{\theta}}(t,T_{ti},S_t) - F_{t,T_{ti}})^2 \tag{7.141}$$

Xu (2004) estimates the risk-neutral parameters for the one-factor mean-reverting model with seasonality ($r = 0$) by minimizing (7.141) using artificial and real data (Henry Hub prices from January 2, 1992 to December 30, 1999), shown in Table 7.7.

The estimated seasonality parameters for model (7.133) (for $r = 0$, $1/2$, and 1) are given in Table 7.8[51] where 0 is used to denote values for some value less than $1e-10$.

Table 7.7

	For artificial data			For real data
	Given	Mean of Est.	Std. of Est.	Est.
$\tilde{\alpha}$	0.0070	0.0070	1.4569e-13	0.0073
$\tilde{L}$	1.7000	1.7000	1.8859e-11	1.6663

Source: Xu (2004).

Table 7.8

	For artificial data			For real data
	Given	Mean of Est.	Std. of Est.	Est.
b	0.0003	0.0003	0	0.0003
β_1	0.1500	0.1500	0	0.1639
β_2	0.0500	0.0500	0	0.0558
η_1	-0.0500	-0.0500	0	-0.0468
η_2	-0.0300	-0.0300	0	-0.0295

Source: Xu (2004).

Two-Factor Model Calibration

Calibration in a two-factor model is an extension of calibration for a one-factor model. First, we "excavate" the hidden things, including the seasonal term $f(t)$ and the long-term mean-reversion factor L_t by matching the actual futures prices with the theoretical futures prices.[52] In this process, we can obtain X_t, parameters for $f(t)$ and some risk-neutralized parameters. Second, with the known X_t and L_t's values, we get parameters in these two stochastic processes by the maximum likelihood (ML) method.[53]

To find the hidden factor L_t and seasonal term $f(t)$ from futures prices, let

$$A_i = f(T_{ii}) + e^{\tilde{\alpha}(t-T_{ii})}(S_t - f(t)) + \frac{\widetilde{\mu}\widetilde{\gamma}}{\widetilde{\alpha}-\widetilde{\mu}}(e^{\tilde{\mu}(t-T_{ii})} - 1)$$

and

$$B_i = \frac{\widetilde{\alpha}}{\widetilde{\alpha}-\widetilde{\mu}}(e^{\tilde{\mu}(t-T_{ii})} - e^{\tilde{\alpha}(t-T_{ii})}).$$

Then by equation (7.138), we have the futures price function $F^{\tilde{\theta}}(t, T_{ii}, S_t) = A_i + B_i L_t$. Notice that the futures price function involves not only $[\widetilde{\alpha}, \widetilde{\mu}, \widetilde{\gamma}]$ and L_t, but also $f(t)$; hence, we can get all of them by matching futures prices.

Here, we let $\widetilde{\theta} = [\widetilde{\alpha}, \widetilde{\mu}, \widetilde{\gamma}, b, \beta_1, \ldots, \beta_N, \eta_1, \ldots, \eta_N]$ In the same way as before, L_t can be defined as a function of $\widetilde{\theta}$:

$$L_t(\widetilde{\theta}) = \frac{\sum_{i=1}^{m}(B_i F_{t,T_{ii}} - A_i B_i)}{\sum_{i=1}^{m} B_i^2} \tag{7.142}$$

Then we free $\widetilde{\theta}$ to obtain the optimal one by

$$\widetilde{\theta} = \arg \min_{\widetilde{\theta} \in \Re^{n0}} \sum_{t=1}^{n} \sum_{i=1}^{m} (F^{\widetilde{\theta}}(t, T_{ti}, S_t, L_t(\widetilde{\theta})) - F_{t,T_{ti}})^2 \tag{7.143}$$

where n_0 is the vector length of $\widetilde{\theta}$. With the obtained $\widetilde{\theta}$, $\{L_t\}_{t=1}^n$, $\{f(t)\}_{t=1}^n$, and hence $\{X_t\}_{t=1}^n$ are all easily computed.

Table 7.9 shows the estimation of risk-neutral parameters of (7.138) for artificial and real data of Henry Hub prices.

Figure 7.22 shows the real and estimated seasonal term based on minimizing the sum of squares of the differences of the two-factor model is (7.143) for Henry Hub actual price data.

Figure 7.23 shows the estimated spot price X_t and long-term mean-reversion parameter L_t of the model using real data.

Xu (2004) estimates the parameters of the model in (7.134) for both artificial and real data using Henry Hub prices from January 2, 1992 to December 30, 1999. When $r = 0$ in equation (7.134), the parameters are given in Table 7.10.

When $r = 1/2$, the parameters are given in Table 7.11.

The parameters of the seasonal factor for all three models (e.g.,$r = 0$, $1/2$, and 1) are shown in Table 7.12.

Figure 7.24 shows the fit of gas futures matching (by optimizing (7.143) between actual and estimated futures prices using a two-factor model with seasonality.

In the middle plot, the bold curve is the real futures curve. The thinner curve is the graph of the futures function given by (7.138). In the lower plot, the bold curve is the real futures curve. The thinner curve is the values of 250 paths of S_t simulated by equation (7.134), where the risk-neutral parameters shown in Table 7.5 are plugged in, and $r = 1$. For comparison, the upper plot shows the seasonal term $f(t)$ (solid curve), and the seasonal volatility function $\sigma(t)$ (dashed curve).

For analysis of the long-run behavior and forecasting of natural gas prices (as well as oil and coal) using stochastic dynamics of the price evolution, see Pindyk (1998). Pinkyk (1998) estimates various models using Kalman filter methods. Pindyk shows that under a theory of depletable resource production and pricing using the actual behavior of real prices over the past century, nonstructural models should incorporate mean-reversion to a stochastically fluctuating trend line that reflects long-run (total) marginal cost, which is unobservable.[54]

Table 7.9

	For artificial data			For real data
	Given	Mean of Est.	Std. of Est.	Est.
$\tilde{\alpha}$	0.0110	0.0110	0	0.0111
$\tilde{\mu}$	0.0020	0.0020	0	0.0018
$\tilde{\gamma}$	2.0000	2.0000	0	2.0028

Source: Xu (2004). Reproduced with permission.

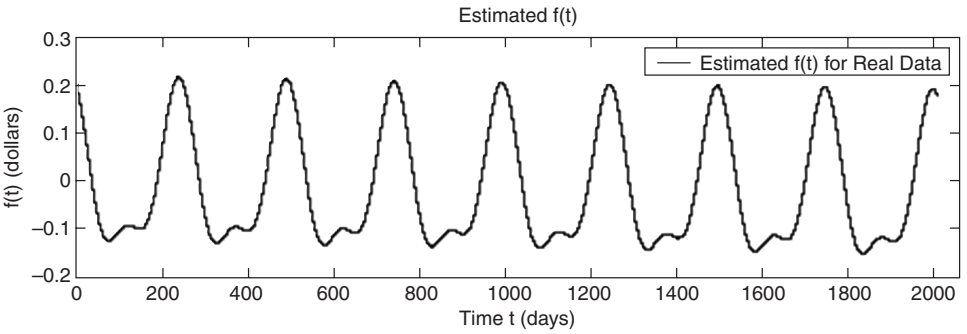

Figure 7.22 *Source: Xu (2004). Reproduced with permission.*

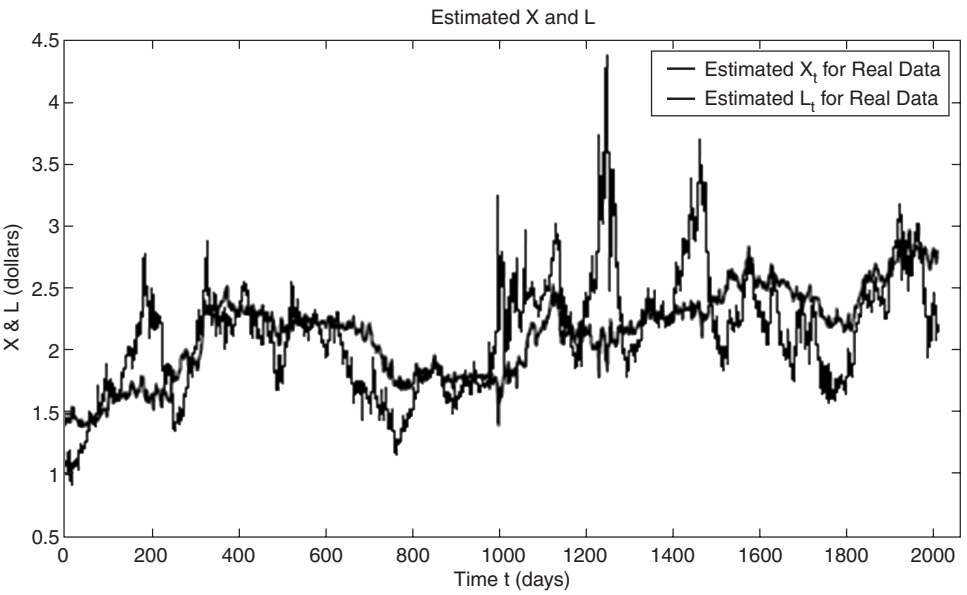

Figure 7.23 *Source: Xu (2004). Reproduced with permission.*

Table 7.10

	For artificial data			For real data
	Given	Mean of Est.	Std. of Est.	Est.
α	0.0240	0.0252	0.0045	0.0244
c	-2.6000	-2.6025	0.0180	-2.5616
λ_1	0.4000	0.4021	0.0203	0.4105
λ_2	0.0800	0.0777	0.0267	0.0790
ω_1	-0.2000	-0.7983	0.0202	-0.4982
ω_2	-0.0700	-0.0683	0.0231	-0.0660
μ	0.0050	0.0068	0.0030	0.0048
τ	0.0300	0.0299	0.0004	0.0329
γ	2.3000	2.2833	0.1297	2.2860

Source: Xu (2004).

Table 7.11

	For artificial data			For real data
	Given	Mean of Est.	Std. of Est.	Est.
α	0.0220	0.0230	0.0048	0.0221
c	-3.0000	-3.0030	0.0169	-2.9894
λ_1	0.3800	0.3787	0.0212	0.3791
λ_2	0.0750	0.0743	0.0198	0.0748
ω_1	-0.1800	-0.1828	0.0229	-0.1826
ω_2	-0.0300	-0.0333	0.0224	-0.0317
μ	0.0050	0.0075	0.0037	0.0050
τ	0.0230	0.0228	0.0004	0.0230
γ	2.3000	2.2866	0.1419	2.2793

Source: Xu (2004).

Table 7.12

	For artificial data			For real data
	Given	Mean of Est.	Std. of Est.	Est.
b	-0.0001	-0.0001	0	-1.4476e-5
β_1	0.1500	0.1500	0	0.1483
β_2	0.0600	0.0600	0	0.0574
η_1	-0.0500	-0.0500	0	-0.0527
η_2	-0.0300	-0.0300	0	-0.0292

Source: Xu (2004).

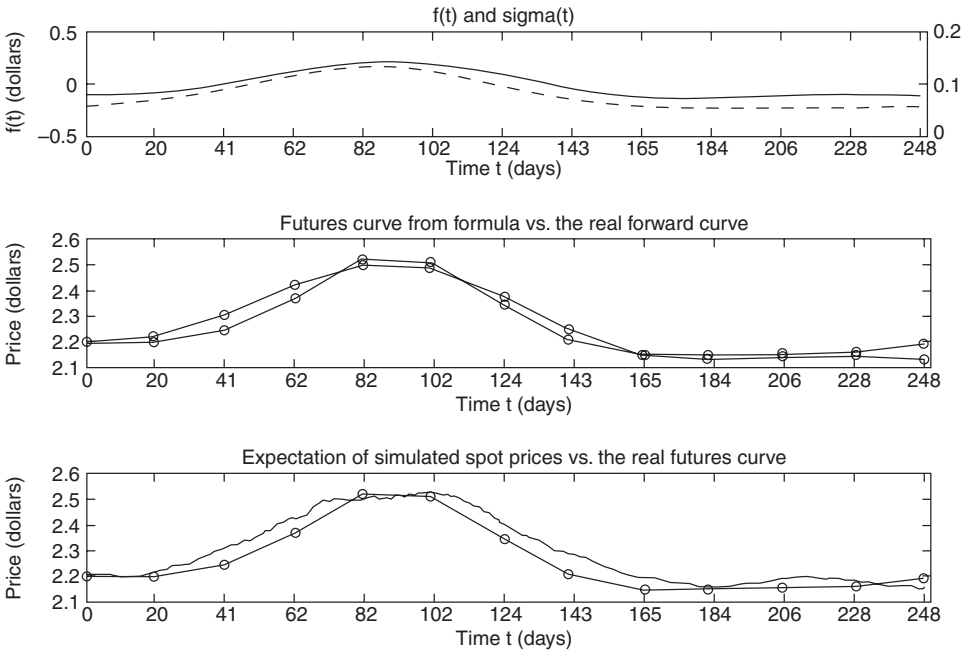

Figure 7.24 *Source: Xu (2004). Reproduced with permission.*

7.17 Natural Gas Pricing in Matlab

Refer to Appendix B to see the full listing of the key Matlab code, written by James Xu (2004), for pricing of natural gas futures using real-time gas data.

7.18 Natural Gas and Electricity Swaps

When one or both parties in a market face a spot market price that differs from the price in a reference market, basis risk may emerge. To manage this risk, forwards and futures contracts cannot be used because they work only for price certainty in a unified market. Instead, other derivative contract instruments like a basis contract may be needed to manage the resulting basis risk. Basis swaps, which are common in natural gas markets, are used to manage this risk. A basis swap allows an individual to lock in a fixed price at a location other than the delivery point of the futures contract. This can be done either as a physical or a financial deal. The most widely used natural gas futures market calls for delivery at the Henry Hub price in Louisiana. Basis contracts are available in the OTC markets to hedge locational, product, and even temporal differences between exchange-traded standard contracts and the particular circumstances of contract users. For example, suppose a local distribution company (LDC) in Tennessee can enter into a swap contract with a natural gas producer, using the Henry Hub prices as the reference price; however,

the LDC would lose price certainty if the local spot market price differed from the Henry Hub price, as shown in Figure 7.25.

In this example, when the Henry Hub price is higher than the Tennessee price by more than it was at the initiation of the swap contract, the LDC gains, because its payment from the producer will exceed the amount it pays to buy gas in its local market.[55] Effectively, the LDC will pay less per thousand cubic feet than the fixed amount the LDC pays the producer. Conversely, if the Tennessee price is lower, the producer's payment will not cover the LDC's gas bill in its local market. In a natural gas basis swap, the OTC trader would pay the LDC the difference between the Tennessee price and the Henry Hub price (for the nominal amount of gas) in exchange for a fixed payment. The variety of contractual provisions is unlimited. For example, the flexible payment could be defined as a "daily or monthly average (weighted or unaveraged) price difference; it could be capped; or it could required the LDC to share the costs when the contract's ceiling price is exceeded."[56] What this OTC contract does is to close the gap between the Henry Hub price and the price on the LDC's local spot market, allowing the LDC to achieve price certainty.

The traders supplying basis contracts can survive only "if the basis difference they pay—averaged over time and adjusted for both financing charges and the time value of money—is less than the fixed payment from the LDC."[57] Competition among OTC traders can only reduce the premium for supplying basis protection. Reducing the underlying cause of volatile price differences would "require more pipeline capacity, more storage capacity, cost-based transmission pricing, and other physical and economic changes to the delivery system itself."[58]

Similarly, in the electricity futures markets, most firms have price exposure at delivery points such as COB, Palo Verde, as well as the PJM Interconnect and other locations. Thus, a firm that uses the NYMEX futures contract to manage price risk at other locations is exposed to basis risk—price differences at different locations. Traders and firms can use basis swaps and contracts to hedge their risk. Basis markets have evolved, allowing firms to hedge risks at most major trading points in the United States and Canada. These

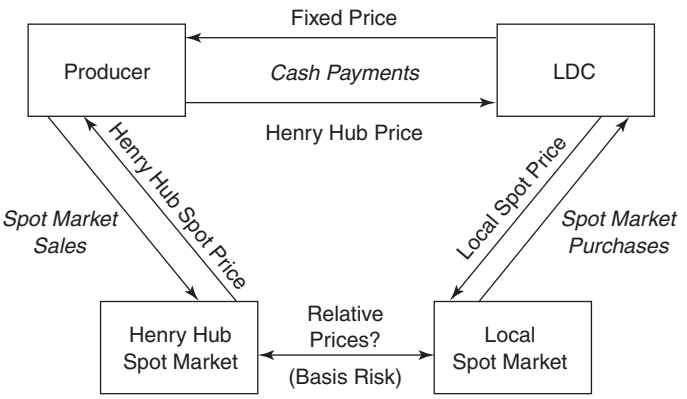

Figure 7.25 *Source: Energy Information Administration/ Derivatives and Risk Management in Energy Industries, U.S. Department of Energy (2002).*

basis markets are quite liquid, with narrow bid offer spreads (typically less than $0.02, but can be wider during volatile periods) and the ability to trade substantial volumes. Basis markets have also begun to develop in the electricity markets in the Western U.S. (e.g., COB, Palo Verde, and Mid-Columbia). Basis markets need not be physically connected by transmission wire or pipeline. For example, there is a Sumas natural gas basis market, even though it would be extremely hard to move gas from this point to the Henry Hub. Following Stoft, Belden, Goldman, and Pickle (1998), we illustrate financial transactions for different users to show the mechanics of these basis swaps.

Generator

To lock in an electricity price in Denver, a generator could sell a futures contract (or a price swap) and a basis swap (see Figure 7.26). Assume that the generator sells a futures contract for $18/MWh for delivery in six months and sells a basis swap agreeing to pay the Denver spot price in exchange for the COB price plus a premium. In six months, the generator sells electricity in Denver and receives the Denver spot price (B), pays the Denver spot price (B) to the basis counterparty, receives the COB spot price (A) plus a fixed premium from the counterparty, and buys a futures contract for the COB spot price (A). All of these transactions cancel out, and the generator should expect to receive the fixed price for the original futures contract, $18/MWh, in addition to the premium received from the basis counterparty. The preceding example represents a financial transaction. Physical transactions are also possible, where the generator provides power to the basis swap counterparty in return for the COB spot price plus a premium.

One risk associated with these transactions is that the generator may be unable to buy a futures contract at COB for the futures price used in the basis swap transaction. One way to avoid this risk is to use price swaps rather than futures contracts.The generator then pays

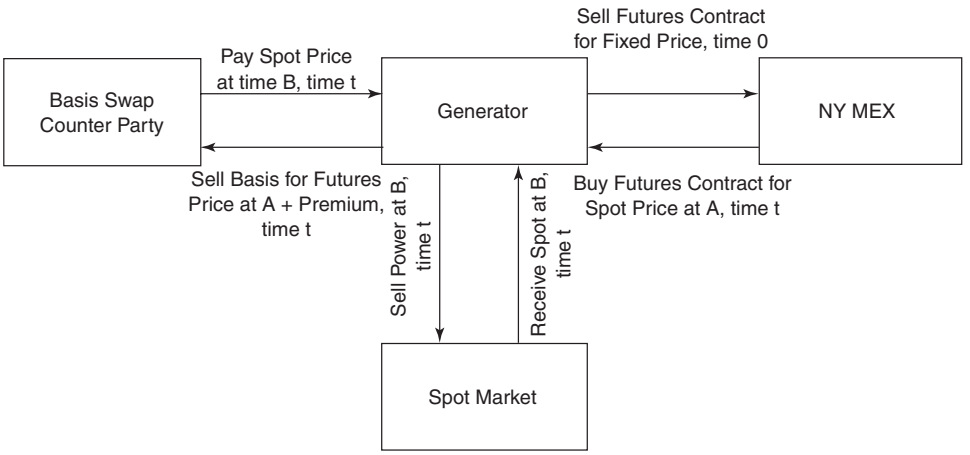

Figure 7.26 *Source: Stoft, S., Belden, T., Goldman, C., and Pickle, S. (1998), 35.*

the price swap counterparty the average of the Dow Jones COB Index, which would cancel out the average of the Dow Jones COB Index from the basis counterparty.[59]

End User

To lock in a fixed price for electricity in Denver, an end user would buy a futures contract (or price swap) and a basis swap (see Figure 7.27). Assume that the end user buys a futures contract for $18/MWh and agrees to pay the COB spot price plus a premium in return for the variable spot market price in Denver. The end user can execute this agreement physically or financially. In either case, the end user locks in an electricity price of $18/MWh plus the premium. The end user can also buy a price swap, rather than a futures contract, to lock in the price in Denver or other locations.

In a price swap, the buyer of the swap agrees to pay a fixed price, which is negotiated at the time of the transaction, and receive a price equal to the simple average of a given month's nonfirm, on-peak, COB index price published in the *Wall Street Journal*.[60] Although swaps can trade in any size, they are typically traded in increments of 25 MW on-peak. Because peak hours in the western United States include 16 hours per day (6 AM to 10 PM), six days a week (Monday through Saturday), the total notional volume equals the number of MWs multiplied by the number of days in the month (excluding Sundays and holidays), multiplied by 16. Just like the buyer of a future, the buyer of a swap profits when prices increase and loses when prices decrease relative to the fixed payment level. When the average of the on-peak Dow Jones COB prices exceeds the fixed price, the buyer of the swap (the fixed price payor) receives a positive cash flow from the transaction. When the average of the on-peak Dow Jones COB prices is below the fixed price, the seller of the swap receives a positive cash flow from the transaction. Swaps can be used to hedge or to speculate.

For example, to lock in an electricity price for July 1998, an end user would buy a price swap (see Figure 7.28). Assume that the end user agrees to pay $25/MWh and to

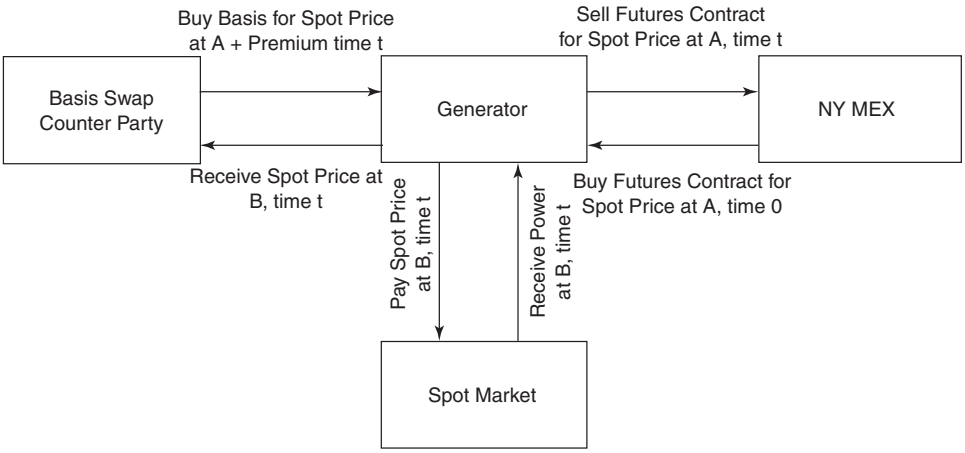

Figure 7.27 *Source: Stoft, S., Belden, T., Goldman, C., and Pickle, S. (1998), 35.*

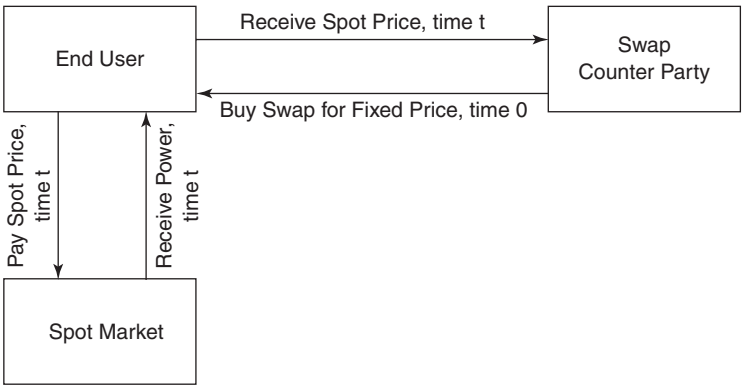

Figure 7.28 *Source: Stoft, S., Belden, T., Goldman, C., and Pickle, S. (1998), pg. 35.*

receive the average Dow Jones COB price. If the spot price at COB in July 2006 averaged $20/MWh, the end user would buy electricity in the spot market for $20/MWh, would receive $20/MWh from the swap counterparty, and would pay the swap counterparty $25/MWh. Using the price swap, the end user has a guaranteed electricity price of $25/MWh, but would be unable to take advantage of the lower-priced electricity if the price were to fall below $25/MWh.

Marketers can also execute these transactions on behalf of generators and end users in order to guarantee them a fixed price at a location other than the COB or Palo Verde. Marketers can also act as basis counterparties for generators and end users in these types of transactions. Generators and end users might work through marketers if they are uncomfortable using the financial tools associated with executing these transactions properly.

For a discussion of hedging and speculating in electricity and commodities using swaps and futures, see Stoft, Belden, Goldman, and Pickle (1998) and Schwartz (1997).

ENDNOTES

1. Lucia, J. and Schwartz, E. (2001), pg. 2.
2. Id., pg. 2.
3. Deng, S. (1999), pg. 4.
4. Id., pg. 2. In addition, regulatory issues such as market rules and market structure may also have an impact on the behavior in competitive electricity markets and, consequently, on their differences across countries.
5. Lucia, J. and Schwartz, E. (2001), pg. 2.
6. See EIA Report, Annual Energy Outlook (2002).
7. Dorr, U. (2003), pg. 3.
8. Id., pg. 3.
9. Lucia, J. and Schwartz, E. (2001), pg. 13.
10. Lucia, J. and Schwartz, E. (2001), pg. 15.
11. Id., pg. 15.

12. Id., pg. 15.
13. Lucia, J. and Schwartz, E. (2001), pg. 20.
14. Established in January 1993, and first covering the Norwegian market, the Nord pool is currently a non-mandatory common multinational market that also includes Sweden since January 1996, Finland since June 15, 1998, and the western part of Denmark since July 1, 1999. Nord Pool organizes two markets, a "physical market" (*Elspot*) and a "financial market" (*Eltermin* and *Eloption*) and also provides clearing services. Elspot is a "spot" market where day-ahead electric power contracts are traded for physical delivery for each one of the 24 hours during the following day.

    Every contract in Elspot refers to a load, in megawatt-hours (WHw, 1MWh equals 1000 kWh), during a given hour, and a price per MWh. A price called the system price is fixed separately for each hour for the next day, based on the balance between supply and demand for all participants in the whole market area (the so-called Nordic Power Exchange Area), without considering capacity limits ("bottlenecks") in the grid among countries. A system price can thus be defined as the market clearing price at which market participants trade electricity for the entire exchange area when no transmission constrains apply. It is also used as a reference price in settlements at the Nord Pool's financial market.
15. $S_t = \alpha + \beta D_t + \sum_{t=2}^{12} \beta_t M_{tt} + X_t$ and $\ln S_t = \alpha + \beta D_t + \sum_{t=2}^{12} \beta_t M_{tt} + Y_t$
16. Lucia, J. and Schwartz, E. (2005), pg. 20.
17. Doerr, U. (2003), pg. 14.
18. Id.
19. Id., pg. 14.
20. Id., pg. 1.
21. Id., pg. 1.
22. Id., pg. 1.
23. Doerr, U. (2003), pg. 21.
24. See London (2004) for an implementation in C++ of the LSM applied to American equity options.
25. Doerr, U. (2003), pg. 22.
26. These sums have at most one non-zero addend.
27. See Doerr, U. (2003). Reproduced with permission.
28. Doerr, U. (2003), pg. 25.
29. Doerr, U. (2003), pg. 26.
30. Doerr, U. (2003), pg. 27.
31. The strikes of the downswings were set equal to the strikes of the upswings.
32. Doerr, U. (2004), pg. 34.
33. Deng, S. (1999), pg. 24.
34. Id., pg. 25.
35. Id., pg. 25.
36. See Deng (1999).
37. Deng, S. (1999).
38. Xiong, L. (2004), pg. 26.
39. Reproduced with permission.

40. As $t \to \infty$, there exists a limiting distribution for X_t. The limiting distribution is called the stationary distribution and its Fourier transform is called the stationary characteristic function (see Grimmett, G. and Stirzaker, D. (1982)).
41. Here we use the compound trapezoidal rule to approximate the integral, and $\sum_i^{'}(A_i)$ denotes the sums of the A_i with the first and last term halved.
42. Xiong, L. (2004).
43. Let $\mathbf{A}$, $\mathbf{B}$ be $K\ x\ L, M\ x\ N$ matrices with elements indexed as

$$\begin{aligned} A[k,l], k = 0,1,....,K-1, \qquad & l = 0,1,...,L-1 \\ B[m,n], m = 0,1,....,M-1, \qquad & l = 0,1,...,N-1 \end{aligned}$$

We define the Kronecker product $\mathbf{A} \otimes \mathbf{B}$ to be a KM x LN matrix

$$\mathrm{A} \otimes \mathrm{B} = \begin{bmatrix} A[0,0]\mathbf{B} & A[0,1]\mathbf{B} & \cdots & A[0,L-1]\mathbf{B} \\ A[1,0]\mathbf{B} & A[1,1]\mathbf{B} & \cdots & A[1,L-1]\mathbf{B} \\ \vdots & \vdots & & \vdots \\ A[K-1,0]\mathbf{B} & A[K-1,1]\mathbf{B} & \cdots & A[K-1,L-1]\mathbf{B} \end{bmatrix}$$

with elements

$$(A \otimes B)[m+kM, n+lN] = A[k,l]B[m,n].$$

44. In 1994, NYMEX launched the crack spread contracts. NYMEX treats the crack spread purchases or sales of multiple futures as a single trade for the purposes of establishing margin requirements. The crack spread contract helps refiners to lock in a crude oil price and heating oil and unleaded gasoline prices simultaneously in order to establish a fixed refining margin. One type of crack spread contract bundles the purchase of three crude oil futures (30,000 barrels) with a sale a month later of two unleaded gasoline futures (20,000 barrels) and one heating oil future (10,000 barrels). The 3-2-1 ratio approximates the real-world ratio of refinery output—two barrels of unleaded gasoline and one barrel of heating oil from three barrels of crude oil. Buyers and sellers concern themselves only with the margin requirements for the crack spread contract. They do not deal with individual margins for the underlying trades. (See Energy Information Administration (2002), pg. 22.)
45. Natural gas is a combustible, gaseous mixture of simple hydrocarbon compounds, usually found in deep underground reservoirs formed by porous rock. Natural gas is fossil fuel composed almost entirely of methane, but does contain small amounts of other gases, including ethane, propane, butane, and pentane.
46. Xu, Z. (2004), pg. 7.
47. Xu, Z. (2004), pg. 8.
48. Id.
49. Id., pg. 8.
50. Id., pg. 8.
51. The seasonality estimates are the same for all three models ($r = 0$, $\frac{1}{2}$, and 1) because all three share the same futures price function given by equation (7.139).
52. Xu, Z. (2004), pg. 80.

53. Id., pg. 40.
54. Pindyk, R. (1998), pg. 33.
55. Energy Information Administration (2002), pg. 21.
56. Id., pg. 21.
57. Id., pg. 21.
58. Id., pg. 21.
59. Stoft, S., Belden, T., Goldman, C., and Pickle, S. (1998), pg. 40.
60. Stoft, S., Belden, T., Goldman, C., and Pickle, S. (1998), pg. 35.